Precambrian Research 276 (2016) 178–193

Contents lists available at ScienceDirect

Precambrian Research

journal homepage: www.elsevier.com/locate/precamres

A paleoproterozoic intra-arc basin associated with a juvenile source in the Southern Brasilia Orogen: Application of U–Pb and Hf–Nd isotopic analyses to provenance studies of complex areas

Alice Westin[a,*], Mario C. Campos Neto[a], Chris J. Hawkesworth[b,c], Peter A. Cawood[b], Bruno Dhuime[c], Hélène Delavault[b]

[a] Instituto de Geociências, Universidade de São Paulo, Rua do Lago, 562, Cidade Universitária, São Paulo, Brazil
[b] Department of Earth Sciences, University of St Andrews, North Street, St Andrews KY16 9AL, UK
[c] School of Earth Sciences, University of Bristol, Wills Memorial Building, Queen's Road, Bristol BS8 1RJ, UK

ARTICLE INFO

Article history:
Received 18 August 2015
Received in revised form 2 February 2016
Accepted 7 February 2016
Available online 21 February 2016

Keywords:
U–Pb LA-MC-ICP-MS
Lu–Hf LA-MC-ICP-MS
Nd isotopes
Provenance
Tectonic setting
Continental crust generation

ABSTRACT

Early Proterozoic sedimentary basins are an important record of crust generation processes and consequently a fundamental key to unraveling Earth's evolution through geological time. Sediments within the basins are typically deformed and metamorphosed by subsequent tectonothermal events, which can obliterate their links to source terranes. Nd-whole-rock and detrital zircon U–Pb and Lu–Hf isotopic analyses are among the most reliable tools to be used in provenance investigations, since zircon is a resilient mineral and the Sm–Nd system is not extensively modified during metamorphism. These methods have been applied to a study of the provenance and tectonic setting of the São Vicente Complex, preserved in a Neoproterozoic passive margin related allochthon within the Southern Brasilia Orogen. The complex consists of siliciclastic and calc-silicate gneisses with mafic and minor ultramafic rocks, which were deformed and metamorphosed during late Neoproterozoic collision between the Paranapanema Block and the São Francisco-Congo plate. Detrital zircons indicate derivation from a juvenile Paleoproterozoic source terrane (peaks of crystallization ages of ca. 2130 Ma, 2140 Ma and 2170 Ma; εHf_t between +0.1 and +6.0; NdT_{DM} = 2.31–2.21 Ga; εNd_t = +1.6 to +2.8), with a minor contribution from older continental crust. Interlayered amphibolite rocks, with juvenile signatures (εHf_t = +5.8 to +8.2; NdT_{DM} = 2.14 and 2.30 Ga; εNd_t = +2.2 and +3.2), yielded similar ages of 2136 ± 17 and 2143 ± 14 Ma, suggesting syn-sedimentary magmatism. Thus, the maximum age of deposition at around 2130 Ma represents the best estimate of the depositional age of the complex. The dominance of detrital zircons ages close to the age of deposition, along with syn-sedimentary magmatism, imply a convergent margin basin tectonic environment for the São Vicente Complex, with similarities to fore arc basin and trench deposits. Amphibolite and meta-sedimentary rocks point to important juvenile magmatism around 2.14 Ga. Juvenile Rhyacian (ca. 2.1 Ga) granite-granodiorite-tonalite orthogneisses with arc-related geochemical signatures (Pouso Alegre Complex) that override the São Vicente Complex, are the probable main source of detritus within the complex. Both basin and source were part of the southern edge of the São Francisco plate during the assembly of West Gondwana, and served as sources for early Neoproterozoic passive margin related basins. The age of intrusive anorogenic A-type Taguar granite indicates that by 1.7 Ga the São Vicente Complex was in a stable tectonic environment.

1. Introduction

Provenance studies of sedimentary basins, even when metamorphosed, provide an important constraint on tectonic setting as well as the evolution of the continental crust (Bhatia and Crook, 1986; Cawood, 1991; Cawood et al., 2012; Dhuime et al., 2011; Dickinson and Suczek, 1979; Hawkesworth et al., 2010; Taylor and McLennan, 1985). However, the determination of the provenance and tectonic setting of basins in tectonically complex areas, subjected to subsequent deformation and metamorphic events, can be hindered by the masking or destruction of original mineral assemblages, sedimentary structures and primary stratigraphic relations, including separation of the basin from its original source. Zircon, due to its physicochemical resilience during deposition and metamorphic

* Corresponding author. Tel.: +55 2111993212464.
E-mail address: alice.teixeira@usp.br (A. Westin).

http://dx.doi.org/10.1016/j.precamres.2016.02.004
0301-9268/

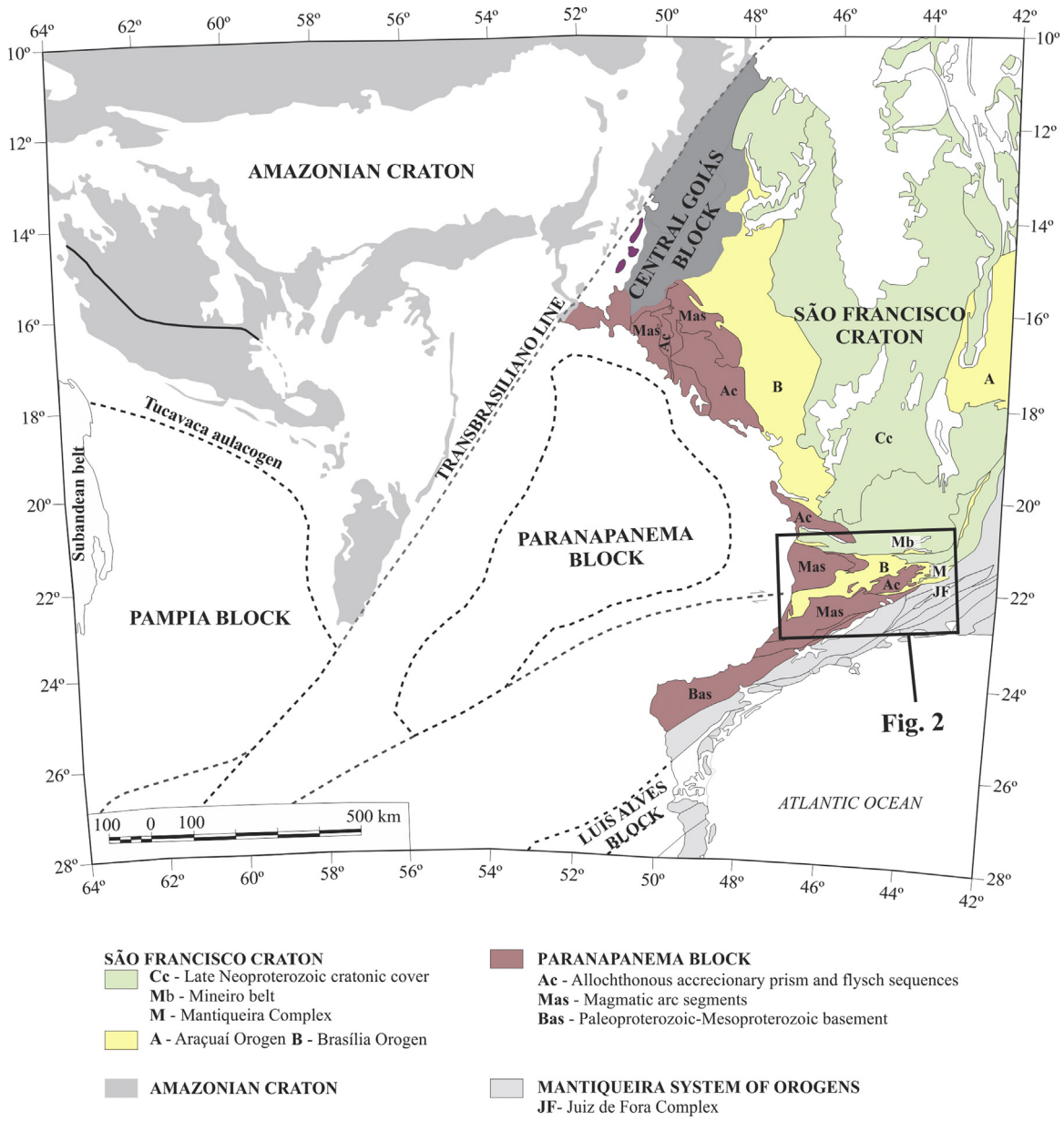

Fig. 1. Tectonic map showing the configuration of the São Francisco Craton and Paranapanema Block. The Amazonian and Luis Alves cratons and Central Goiás and Pampia blocks have been inserted to contextualize the studied area. (For interpretation of the references to color in this figure legend, the reader is referred to the web version of the article.)

Source: Modified from the Geological Map of South America (Commission for the Geologial Map of the World, 2001) and Westin and Campos Neto (2013).

events, enables the determination of crystallization age and isotopic signature of source rocks through U–Pb and Lu–Hf analyses (Cawood and Nemchin, 2001; Cawood et al., 2012, 2007; Condie et al., 2005; Dhuime et al., 2011; Dickinson and Gehrels, 2009; Hanchar and Hoskin, 2003; Hawkesworth and Kemp, 2006). Thus, study of detrital zircons has proven to be an important technique in provenance studies and in linking basins to probable source regions. Allied to detrital zircon analysis, the use of whole-rock Nd isotope compositions of the basin strata can help reveal the role of crustal and juvenile sources during sediment accumulation (McCulloch and Wasserburg, 1978; McLennan et al., 1990). Furthermore, petrographic, isotopic and geochemical signatures of igneous rocks within the basin succession can provide better information on the time of deposition, deformation and the tectonic setting of the basin (Barbarin, 1999; Pearce and Stern, 2006; Pupin, 2000, 1980; Sun and McDonough, 1989).

The southern segment of the Brasilia Orogen provides an example of how U–Pb detrital ages and Nd–Hf isotopic compositions can be applied to discriminate different sedimentary basins and their probable sources and tectonic environments. The orogen runs along the southern margin of São Francisco Craton (Fig. 1) and it comprises three distinct paleogeographic domains: passive margin, fore-arc/accretionary prism and magmatic arc (Campos Neto, 2000; Campos Neto et al., 2011). Therefore, the combination of field mapping with isotopic signatures of rocks, and detrital and magmatic zircons are among the most reliable tools to investigate the provenance and tectonic setting of this complex area. Additionally, the presence of diverse potential sources with similar ages around the area (e.g. ~2.1 Ga orthogneisses and granitoids in allochthons related to passive and active margins) ensures that the association between different isotopic analyses remains a key approach.

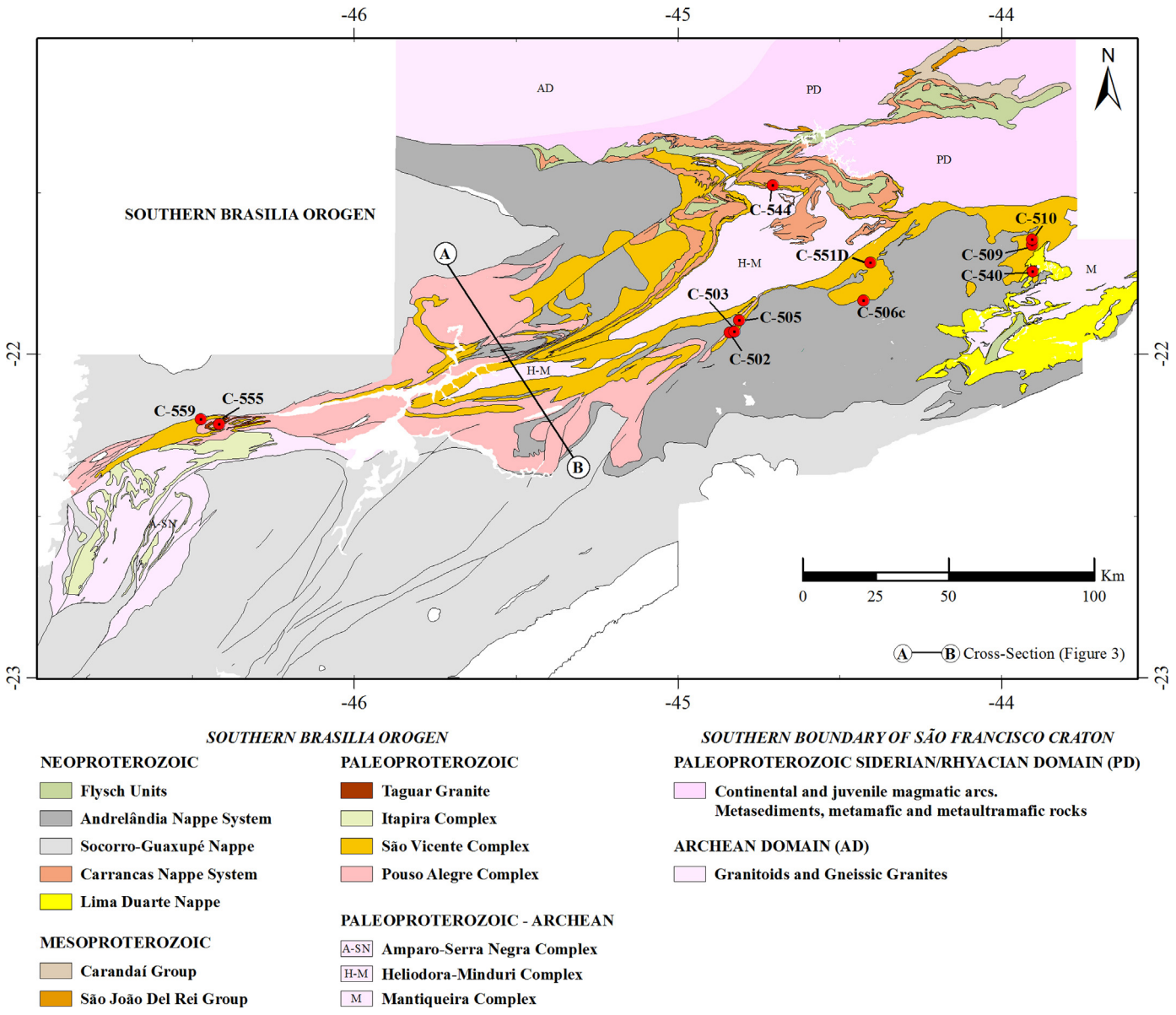

Fig. 2. Geological map of the Southern Brasília Orogen showing the locations of the samples analyzed (see Table 1 for geographic coordinates). Modified from Campos Neto et al. (2010), Gengo (2014), Nunes et al. (2008), Paciullo et al. (2002), Quéméneur et al. (2002), Ribeiro et al. (2002), Trouw et al. (2008, 2002), Vinagre et al. (2014). The outlined contacts are tectonic. (For interpretation of the references to color in this figure legend, the reader is referred to the web version of the article.)

In this contribution we present new isotopic data for metasedimentary and meta-basic rocks that belong to the São Vicente Complex, a passive margin related allochthon of the Southern Brasilia Orogen, and for the related Taguar gneissic granite. The complex was previously interpreted as the basal unit of an early Neoproterozoic (ca. 1000–900 Ma) passive margin basin that developed along the southern margin of the São Francisco paleoplate (Paciullo et al., 2000; Trouw et al., 2000). However, new Paleoproterozoic U–Pb provenance ages and juvenile Nd and Hf data permit new interpretations for the tectonic environment of sedimentation and the probable source rocks for this complex.

2. Geological setting

Passive margin, fore-arc/accretionary prism and magmatic domains belonging to the southern segment of the Brasília Orogen are deformed into a thick-skin stack of nappes (Campos Neto and Caby, 1999; Trouw et al., 2000) that were transported east-northeast, through in-sequence thrusting of the orogenic pile onto the cratonic foreland (Campos Neto et al., 2011). Deformation was driven by the Neoproterozoic collision between the São Francisco-Congo plate (Alkmim et al., 1993; Ussami, 1999) and the Paranapanema block (Mantovani and Brito-Neves, 2005; Mantovani et al., 2005) during assembly of West Gondwana in the Brasiliano/Pan-African Orogeny.

2.1. Magmatic and fore-arc/accretionary prism domains: tectonic units of the Paranapanema Block

The Paranapanema Block corresponds to an active margin domain now covered by the Phanerozoic Paraná Basin (Fig. 1). Deep drilling, geochronology (Brito-Neves et al., 1984; Cordani et al., 1984) and isostatic modeling surveys (Mantovani and Brito-Neves, 2005; Mantovani et al., 2005) have demonstrated the existence of a cratonic core with a deep lithospheric keel, bordered by orogenic belts (Assumpção et al., 2006; Lesquer et al., 1981; Rocha et al., 2011).

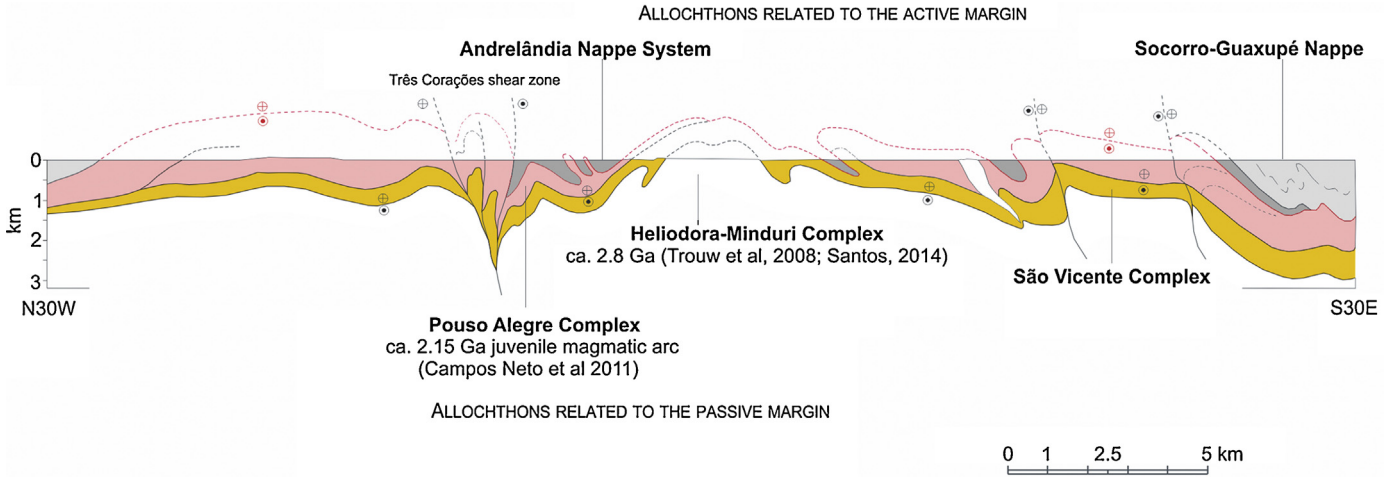

Fig. 3. Section showing the tectonic relation between the allochthons related to the São Francisco Craton (passive margin: Pouso Alegre, São Vicente Complex and Heliodora-Minduri Complexes) and the allochthons related to the Paranapanema Block (active margin: Andrelândia Nappe System and Socorro-Guaxupé Nappe).

The block is dominated by ca. 670–625 Ma meta-granitoid rocks and high-pressure meta-sedimentary units interpreted to represent magmatic arc (Socorro-Guaxupé Nappe) and fore-arc/accretionary prism (Andrelândia Nappe System) segments (Figs. 1 and 2 – Campos Neto and Caby, 2000, 1999; Mora et al., 2014). The basement of the magmatic arc domain comprises an antiformal nucleus of 2.2 Ga orthogneiss at the base, covered and intruded by ca. 1.7–1.8 Ga meta-volcano-sedimentary units and meta-syenites, ca. 1.46 Ga meta-turbidites and meta-basic/meta-volcanic rocks, and a 1.25–0.9 Ga carbonate platform (Fig. 1 – Basei et al., 2008; Campanha and Sadowski, 1999; Campanha et al., 2015; Cury et al., 2002; Faleiros et al., 2011; Henrique-Pinto et al., 2015; Siga et al., 2011).

2.2. *Passive margin domain: tectonic units related to the southern São Francisco Craton and its orogenic margin*

2.2.1. *Neoproterozoic meta-sedimentary sequences*

The Carrancas Nappe System and the Lima Duarte Nappe occur in flat-lying sheets that were transported toward the São Francisco Craton margin (Fig. 2). These sheets lie structurally below the fore-arc/accretionary prism domain of the Paranapanema Block (Figs. 1 and 2; Campos Neto, 2000; Campos Neto et al., 2004; Ribeiro et al., 1995; Trouw et al., 2000). The passive margin succession consists of a transgressive sequence that accumulated around 1000–900 Ma and were metamorphosed between 600–575 Ma (Campos Neto et al., 2011; Ribeiro et al., 1995; Valeriano et al., 2004; Valladares et al., 2004; Westin and Campos Neto, 2013). A regional unconformity separates this transgressive sequence from a meta-wacke unit interpreted as a syn-collisional flysch deposit (Fig. 2 – Santos, 2011; Westin and Campos Neto, 2013). The transition to the cratonic area is marked by Mesoproterozoic sequences (Fig. 2) of quartzites, limestones and pelites represented by the São João del Rei and Carandaí intracratonic basins (Ribeiro et al., 2013).

2.2.2. *Allochthonous and imbricated substratum*

The Archean units, which outcrop in large antiformal cores, comprise migmatitic orthogneisses, dated at 3.0–2.7 Ga, represented by the Amparo-Serra Negra, Heliodora-Minduri and Petunia complexes (Fig. 2 – Campos Neto et al., 2004; Fetter et al., 2001; Noce et al., 2007; Peternel et al., 2005; Pinheiro, 2013; Santos, 2014; Tassinari and Nutman, 2001). The Paleoproterozoic units are represented by the Mantiqueira, Juiz de Fora and Pouso Alegre complexes.

The Mantiqueira Complex occurs as the Lima Duarte Nappe and São Vicente Complex substratum (Figs. 1 and 2) and comprises 2.18–2.04 Ga calc-alkaline orthogneisses with Archean protoliths (Heilbron et al., 2010; Noce et al., 2007).

The Juiz de Fora Complex occurs associated with the Lima Duarte Nappe (Fig. 1) and consists of orthogranulites, predominantly of enderbitic compositions, and basic granulites (Heilbron et al., 2010; Noce et al., 2000) interpreted as an island arc developed during the Rhyacian orogeny (2195–2084 Ma; Heilbron et al., 2010; Noce et al., 2007). It constitutes the basement of the ca. 630–585 Ma Araçuaí orogen magmatic arc, which was accreted to the cratonic margin of the São Francisco-Congo Plate in the Late Neoproterozoic (Noce et al., 2007; Pedrosa-Soares et al., 2008, 2001).

The Pouso Alegre Complex comprises metatexitic granodioritic-tonalite orthogneisses, which have yielded ages of 2.15–2.07 Ga and are associated with coarse-grained porphyroclastic granites and subordinate amphibolites (Campos Neto et al., 2011; Fetter et al., 2001; Peternel et al., 2005; Zuquim et al., 2011). This complex is interpreted as fragments of an island arc due to its juvenile signature (Campos Neto et al., 2011; Cioffi et al., 2016), and it occurs as the substratum of the Andrelândia Nappe System and overriding meta-sedimentary and meta-igneous rocks of the São Vicente Complex (Figs. 2 and 3).

2.2.3. *The São Francisco Craton orogenic margin*

The Mineiro belt strikes NE–SW in the southern wedge of the São Francisco Craton (Figs. 1) and represents successive accretion of oceanic and continental arcs and associated meta-sedimentary sequences (Ávila et al., 2014, 2010; Noce et al., 2000; Teixeira et al., 2000). The igneous suites of the Mineiro belt have ages of 2.35–2.10 Ga and include undeformed plutons of gabbroic to granitic composition as well as orthogneisses of trondhjemitic to granodioritic composition (Barbosa et al., 2015; Seixas et al., 2013, 2012; Teixeira et al., 2015).

2.2.4. *São Vicente Complex*

The São Vicente Complex has previously been mapped as an interstratified meta-sedimentary sequence consisting of a basal biotite gneiss with lithic fragments, and an overlying unit of biotite gneiss, quartzites and schists, having the São Francisco Craton rocks as their main source (Paciullo et al., 1996, 1993). Subsequently it was interpreted as the basal units of a Neoproterozoic depositional sequence (Paciullo et al., 2000; Trouw et al., 2000). Given the pervasive deformation and metamorphism, we interpret the sequence as a geological complex comprising a number

Table 1
Primary field, petrographic characteristics and geographic coordinates of the analyzed samples.

Sample/UTM	Unit/rock type	Mineralogy	Other features
C-551D W561478 S7598586	Epidote-plagioclase-quartz-biotite-gneiss with K-feldspar and carbonate	Biotite + quartz + plagioclase + epidote + muscovite ± microcline ± carbonate ± opaque mineral	Lithic fragments: biotite + plagioclase + microcline + quartz; Quartz feldspathic veins: quartz + plagioclase ± microcline; Muscovite- and myrmekite-rich leucogranite.
C-502 W516564 S7574642	Plagioclase-quartz-biotite-epidote gneiss with K-feldspar and hornblende	Hornblende + epidote + biotite + quartz + plagioclase ± titanite	Porphyroclasts: hornblende (up to 0.5 mm); quartz and fragmented K-feldspar crystals (with perthite texture) (Figs. 5 AI/AII); Sigmoidal-shaped lithic fragments: up to cm-sized (Fig. 4A). Composed mainly by plagioclase + quartz, rimmed by hornblende, biotite and epidote (Figs. 5 BI/BII).
C-503 W517920 S7575084 **C-505** W519581 S7578881	Epidote-plagioclase-biotite-quartz gneiss with carbonate	Quartz + biotite + plagioclase ± epidote ± carbonate	Lithic fragments: quartz + plagioclase, with late carbonate; Quartz-rich felsic lenses: folded and streched (Fig. 4C); Plagioclase porphyroclasts.
C-506c W559198 S7585614	Biotite-plagioclase-quartz schist with garnet	Quartz + plagioclase + biotite ± muscovite ± garnet	Polycrystalline feldspar and quartz (cm size): stretched and parallel to the main foliation (Fig. 4B); Lithic fragments: cm-size, sigmoidal shape; plagioclase + quartz ± biotite.
Quartzite **C-510** W613244 S7606088 **C-559** W347883 S7544195 **Amphibolite** **C-509** W613274 S7604254 **C-540** W613325 S7595159	Paragneiss interbedded with quartzite, muscovite quartzite, muscovite-quartz schist with amphibolite and calc-silicate rocks and minor metaultramafic rocks	Paragneiss: muscovite, biotite, sillimanite and garnet porphyroblasts; Quartzite: quartz + muscovite ± opaque mineral; Amphibolite: hornblende + andesine ± quartz; Metaultramaphic rocks: talc and hornblende + talc + Mg-chlorite; Calc-silicate rocks: andesine/labradorite + quartz + garnet ± biotite ± muscovite ± tourmaline.	Paragneiss: intrafolial folds; quartz-feldspathic lenses; sigmoidal-shaped quartz (up to 10 cm); Quartzite: m-sized lenses; associated with quartzite and muscovite-quartz schist.

of immature meta-sedimentary rocks, associated with calc-silicate rocks and subordinate meta-mafic and meta-ultramafic rocks. The complex occurs beneath the Andrelândia Nappe System and Lima Duarte Nappe, imbricated in the Carrancas Nappe System or as a sheet sandwiched between the Pouso Alegre Complex and Archean orthogneisses (Figs. 2 and 3).

The meta-sedimentary rocks vary from plagioclase and quartz-rich gneisses and schist to muscovite quartzite (see Table 1 for detailed description). Epidote, biotite, muscovite, hornblende, carbonate and K-feldspar occur in varying proportions in the gneiss and schist (Figs. 4 and 5). Calc-silicate rocks and amphibolite rocks occur as layers and *boudins* within the gneisses and the amphibolite can be seen to be associated with meta-ultramafic rocks in the larger outcrops. Gneisses and schist are characterized by the presence of lithic fragments and detrital feldspar and quartz, usually with sigmoidal shapes (Figs. 4 and 5).

3. Analytical methods

3.1. Sm–Nd methodology

Samples were prepared at the laboratories of the NAP GeoAnalítica-USP Core Facility of the Geosciences Institute of the University of São Paulo (IGc-USP) and involved cleaning, comminution in a hydraulic press, quartering, and grinding in a planetary-type agate ball mill. The isotopic data were obtained at the Geochronological Research Center (CPGEO) of the IGc-USP – see Supplementary Table 1 for technical information – and analytical procedures followed Sato et al. (2010). The $^{143}Nd/^{144}Nd$ normalization value of 0.7219 (DePaolo, 1981), $^{143}Nd/^{144}Nd_{CHUR} = 0.512638$ and $^{147}Sm/^{144}Nd_{CHUR} = 0.1967$ (Hamilton et al., 1983) were used for all the analyses.

Seven samples (C-502A, C-503A, C-505A, C-506c, C-510, C-509 and C-540 – Table 1) were analyzed by isotopic dilution using a Thermal Ionization Mass Spectrometry (TIMS), including Sm and Nd ppm concentrations. The $^{143}Nd/^{144}Nd$ mean average of the JNDi standard in the period was 0.512100 ± 0.000008. The isotopic compositions of sample C-559 were determined using an inductively coupled plasma mass spectrometry (ICP-MS). The $^{143}Nd/^{144}Nd$ mean average of the JNDi standard in the period was 0.512095 ± 0.000007 and the analytical blank was 53 pg. For this sample, Sm and Nd concentrations were acquired using a PerkinElmer/Sciex quadrupole-type spectrometer, ELAN 6100DRC model. Analytical protocols followed Navarro et al. (2008), and T_{DM} model ages and εNd (age) values were calculated using GCDkit 3.00 software (Janoušek et al., 2006). All reported errors are at 2 s.d. level.

3.2. U–Pb zircon methodology

We determined crystallization ages by measurement of $^{206}Pb/^{238}U$ and $^{207}Pb/^{235}U$ ratios (and respective 2σ errors) in detrital and magmatic zircon grains extracted from six meta-sedimentary rocks, two meta-basic rocks and a granite sample using a Laser Ablation Multicollector Inductively Coupled Plasma Mass Spectrometer (LA-MC-ICP MS). Heavy-mineral concentration was carried out using a Wilfley table. The separation of magnetic

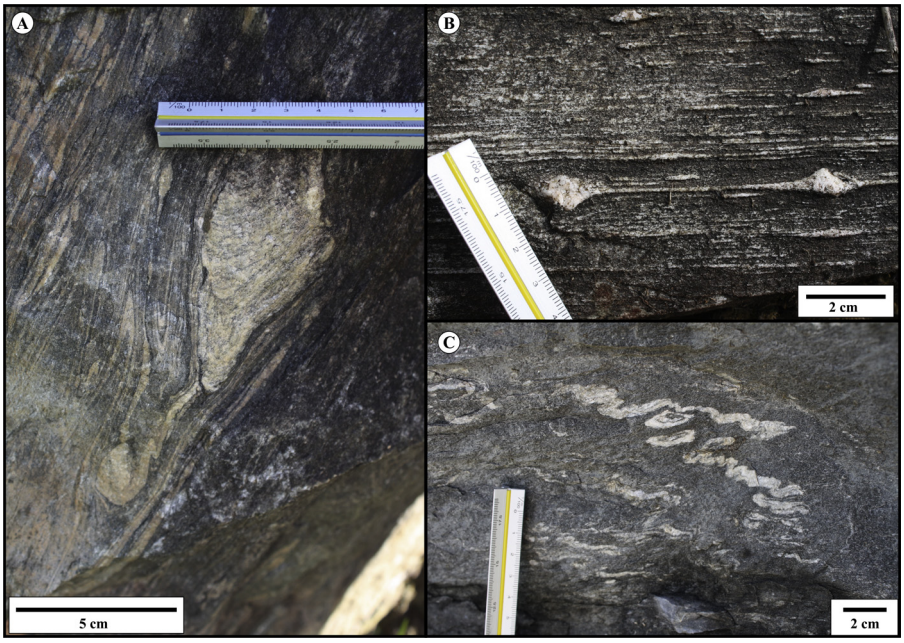

Fig. 4. (A) Plagioclase-quartz-biotite-epidote gneiss with hornblende and K-feldspar porphyroclasts; note the 4 cm × 5 cm feldspathic quartzite lithic fragment. (B) Biotite-plagioclase-quartz schist to quartzite interbedded with garnet-bearing granite; note the feldspar porphyroclasts as stretched sigmoids. (C) Epidote-plagioclase-biotite-quartz gneiss with carbonate. Note the sheath folds in the quartz-rich layers.

minerals by a hand magnet and Frantz-type separator and the separation of minerals with bromoform ($CHBr_3$) and methylene iodide (CH_2I_2) were conducted at NAP GeoAnalítica Core Facility and in the CPGEO Separation Laboratory of the IGc-USP. These steps were followed by crystal collection under a magnifying glass and subsequent mounting using epoxy resin. Cathodoluminescence images were obtained from Au-coated mounts, using a Quanta 250 FEG electron microscope equipped with Mono CL3+ cathodoluminescence spectroscope (Centaurus).

Samples C-502, C-503, C-505, C-506c, C-510, C-509 and C-540 (Table 1) were analyzed at the CPGEO of the IGc-USP and ablation was performed using 25 μm or 30 μm spot sizes (see Supplementary Tables 2–8 for detailed analytical conditions). GJ-1 and NIST-612 were used as analytical standards (Elhlou et al., 2006; Woodhead and Hergt, 2001). Cup configuration allowed simultaneous measurement of ^{206}Pb, ^{208}Pb, ^{232}Th, ^{238}U, ^{202}Hg, ^{204}Pb and ^{207}Pb isotopes. The instrumental drift was corrected by comparing the analytical results for GJ-1 ($^{206}Pb/^{238}U$ mean

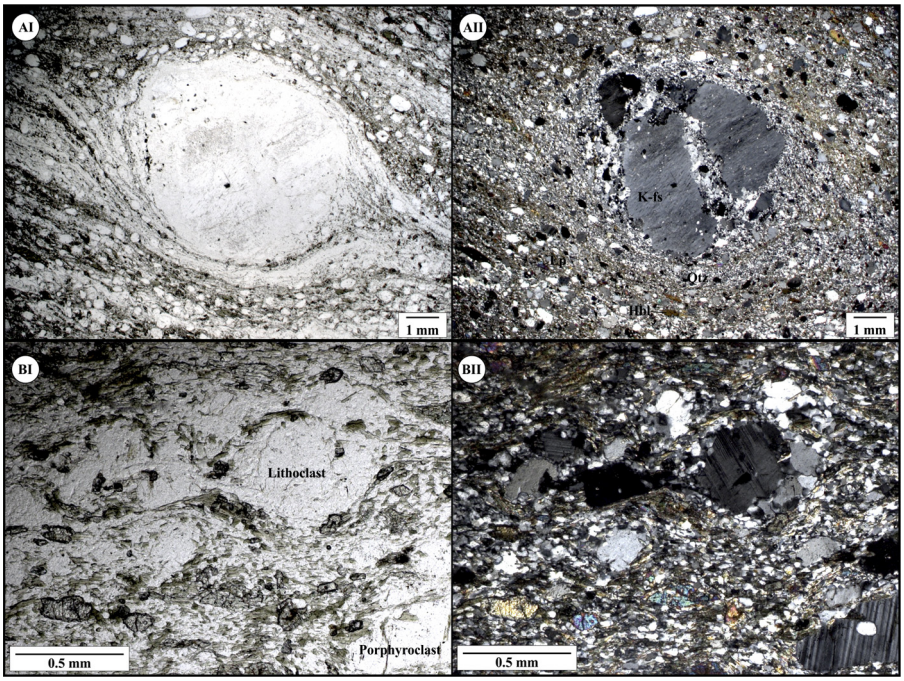

Fig. 5. Photomicrographs showing representative samples. The number I following the letters correspond to photomicrographs taken with plane-polarized light and the number II photomicrographs were taken with cross-polarized light. Abbreviations according to Siivola and Schmid (2007). (AI and AII) Plagioclase-quartz-biotite-epidote gneiss with hornblende and perthitic K-feldspar porphyroclast; (BI and BII) Plagioclase-quartz-biotite-epidote gneiss with hornblende and sigmoidal-shaped lithoclasts and fragments of plagioclase and quartz.

age ± 2σ error = 599 ± 10 Ma) and NIST-612 ($^{204}Pb/^{206}Pb$ mean ratio = 0.051; $^{207}Pb/^{206}Pb$ mean ratio = 0.830; $^{208}Pb/^{206}Pb$ mean ratio = 2.197) with reference values. The net ion signals were obtained via subtraction of the background contribution, and common Pb corrections (Stacey and Kramers, 1975) were performed by measuring the ^{204}Pb isotope, after accounting for ^{204}Hg interference (assuming a $^{202}Hg/^{204}Hg$ ratio of 4.355) (Sato et al., 2010). Finally, the $^{206}Pb/^{238}U$, $^{207}Pb/^{235}U$ and $^{206}Pb/^{207}Pb$ ratios, and respective errors, were calculated and "Rho" values computed. All reported errors are at 2 s.d. level. Data reduction used an in house spreadsheet.

Samples C-559 and C-555 (Table 1) were analyzed at the Geochronology Laboratory of the University of Brasília (GL-UnB) and ablation was performed using 25 μm or 30 μm spot sizes (see Supplementary Tables 9 and 10 for detailed analytical conditions). GJ-1 ($^{206}Pb/^{238}U$ mean age ± 2σ error = 535 ± 6 Ma) was used as an analytical standard (Elhlou et al., 2006). Details on analytical procedures are given by Bühn et al. (2009) and data reduction used an in house spreadsheet (Oliveira et al., 2014). All reported errors are at 2 s.d. level.

The U–Pb results were processed using Isoplot 4.15 software (Ludwig, 2008), for U–Pb Concordia diagrams and Probability Density Plots, and Density Plotter program (Vermeesch, 2012), for Kernel density estimate. Analyses with discordance greater than 5% and common lead greater than 3% were discarded.

3.3. Lu–Hf zircon methodology

Lu–Hf isotopes were measured at the University of Bristol (Bristol Isotope Group) using a ThermoFinnigan Neptune multicollector inductively-coupled plasma mass spectrometer (MC-ICP-MS) coupled with a Photon-Machine Analyte G2 Excimer laser (193 nm wavelength) (see Supplementary Table 11). Samples C-502, C-505, C-506c, C-509, C-510 and C-559 (Table 1) were analyzed and ablation was performed using a 50 μm spot size at the same location as the U–Pb site. Laser frequency was 5 Hz and the energy density of the laser beam was ca. 6 J/cm^2. A typical analysis was 90 s, including a 30 s background measurement and a 60 s ablation period. Correction for the interferences and mass bias followed the Bristol routine procedure (Hawkesworth and Kemp, 2006; Kemp et al., 2009). The correction for the isobaric interference of Yb and Lu on ^{176}Hf was made following a method detailed in Fisher et al. (2011). For Yb, the interference-free ^{171}Yb was corrected for mass bias effects using an exponential law and $^{173}Yb/^{171}Yb = 1.130172$ (Segal et al., 2003). The mass bias-corrected ^{171}Yb was monitored during the run and the magnitude of the ^{176}Yb interference on ^{176}Hf was calculated using $^{176}Yb/^{171}Yb = 0.897145$ (Segal et al., 2003). For Lu, the interference-free ^{175}Lu was corrected for mass bias effects assuming $\beta Lu = \beta Yb$ and using an exponential law. The mass bias-corrected ^{176}Lu was monitored during the run and the magnitude of the ^{176}Lu interference on ^{176}Hf was calculated using $^{176}Lu/^{175}Lu = 0.02655$ (Vervoort et al., 2004). Interference-corrected $^{176}Hf/^{177}Hf$ were corrected for mass bias using an exponential law and $^{179}Hf/^{177}Hf = 0.7325$ (Patchett et al., 1981), and were finally normalized to JMC-475 = 0.282160. The accuracy and long-term reproducibility of the measurements were gauged by analysing two zircon reference standards: Plesovice ($^{176}Hf/^{177}Hf = 0.282472 \pm 21$, $n = 24$) and Mud Tank ($^{176}Hf/^{177}Hf = 0.282504 \pm 20$, $n = 21$) (all errors at 2 s.d. level).

4. U–Pb results

Most of the zircon crystals from the gneisses vary from prismatic to equidimensional and are idiomorphic to subidiomorphic, with pyramidal terminations or rounded and with magmatic internal zoning (Fig. 6). Rounded crystals without internal zoning are rare and resorption textures and xenocrystic cores are common (Corfu et al., 2004). The zircon grains from the muscovite quartzites are similar to those from the gneisses, although these rocks have more rounded crystals with concentric zoning. The majority of zircon crystals have thin overgrowths, inferred to be related to metamorphism associated with the Neoproterozoic collision.

All the zircons from the meta-sedimentary rock samples align along a lead loss discordia with an upper intercept around 2100 Ma and a lower intercept in the Neoproterozoic, around 594 ± 57 Ma. The lower intercept is consistent, within error, with the 549 ± 17 Ma obtained from a crystal overgrowth in sample C-510 (Supplementary Table 6) and with the 590–570 Ma metamorphism determined for the passive margin-related allochthons (Campos Neto et al., 2011; Machado et al., 1996; Valeriano et al., 2004). Therefore the lead loss is interpreted to has been caused by the Neoproterozoic tectonothermal event that affected these rocks.

Samples C-503 and C-505, which belong to epidote-plagioclase-biotite-quartz gneiss with carbonate and sample C-506c, a biotite-plagioclase-quartz schist, yielded age peaks around 2130 Ma (Fig. 7). Sample C503 has detrital zircon ages in the range from 2232 Ma to 2107 Ma ($n = 40$), with individual 2σ errors ranging from 11 to 62. The probability density plot shows a younger age peak of ca. 2130 Ma and a slightly older age peak around 2150 Ma, besides two detrital crystals with ages of 2232 ± 62 Ma and 2203 ± 21 Ma (Fig. 7). One crystal with an age of 2175 Ma was disregarded due to its higher U content (215 ppm) when compared to the other crystals, perhaps due to Pb loss. Sample C-505 only has one age peak of ca. 2130 Ma (Fig. 7), with detrital ages ranging from 2178 Ma to 2112 Ma ($n = 27$), with individual 2σ errors varying from 19 to 42 Ma. Sample C-506c has a detrital age pattern similar to sample C-505, with detrital zircon ages ranging from 2145 Ma to 2099 Ma ($n = 15$; individual 2σ errors = 13–19), and an age peak of ca. 2130 Ma (Fig. 7).

Samples C-510 and C-559 from muscovite quartzite interbedded with muscovite-quartz schist, paragneiss, amphibolite and calc-silicate rocks, and sample C-502 of plagioclase-quartz-biotite-epidote gneiss with K-feldspar and hornblende, yielded age peaks of 2170 Ma and 2140 Ma. Sample C-559 has detrital zircon ages ranging from 2227 Ma to 2113 Ma ($n = 12$; individual 2σ errors = 12–45), with an age peak of ca. 2140 Ma (Fig. 7). Sample C-502 also yielded an age peak of ca. 2140 Ma, with detrital ages in the range of 2173 Ma and 2110 Ma ($n = 33$; individual 2σ errors from 10 to 24; Fig. 7). Sample C-510 has a main group of detrital ages in the range 2248 Ma and 2099 Ma ($n = 47$; individual 2σ errors = 11–39), with age peaks of ca. 2170 Ma and 2140 Ma (Fig. 7). An age peak of ca. 2100 Ma was disregarded because it is based on a single zircon crystal of 2099 ± 11 Ma, and so it is not statically representative. This sample also yielded four Archean detrital crystals of 2895 Ma, 2894 Ma, 2814 Ma and 2695 Ma, although the 2814 Ma zircon was rejected due to its higher U content (246 ppm) when compared to the other Archean crystals (U = 133–195).

Two crystals with ages of 2030 ± 20 Ma (sample C-503) and 2044 ± 25 Ma (sample C-510) were also analyzed. Though these crystals have concordance higher than 95%, the higher U contents of 168 ppm and 229 ppm could indicate a process of Pb loss. Therefore, these younger ages were disregarded for the final interpretations.

Because of the Pb loss due to the Neoproterozoic tectonothermal event, the maximum depositional ages of the meta-sedimentary rocks were determined using the youngest age peaks observed in the Probability Density Plots (Fig. 7). The youngest individual crystal age may have been compromised by Pb loss, or it may represent part of a cluster of overlapping ages (Dickinson and Gehrels, 2009; Gehrels, 2013).

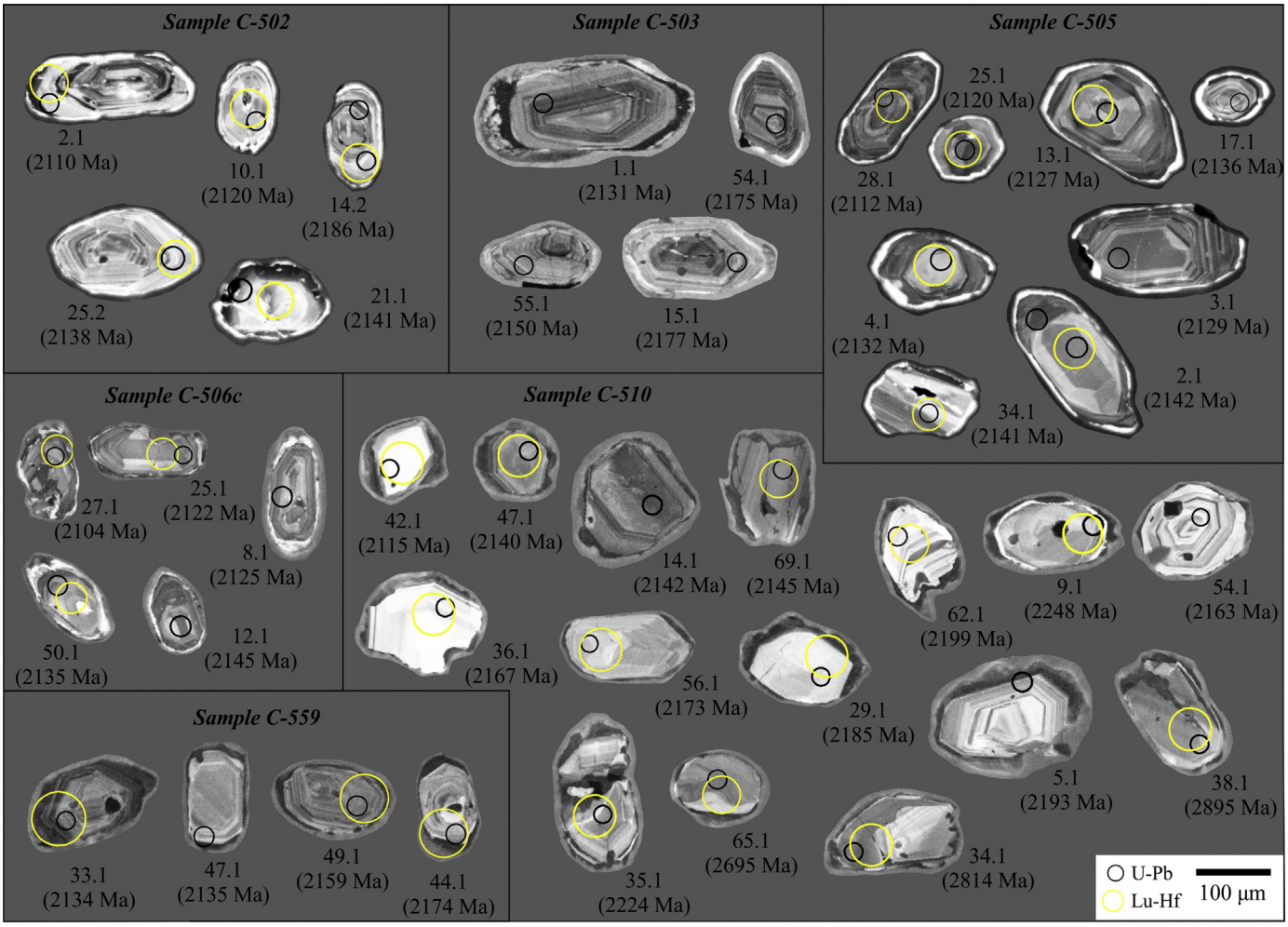

Fig. 6. Cathodoluminescence images of representative zircon crystals from meta-sedimentary samples. The small black circles represent spots analyzed for U–Pb isotopes while the larger yellow circles are those for Lu–Hf analyses. (For interpretation of the references to color in this figure legend, the reader is referred to the web version of the article.)

5. Nd and Hf isotopic analyses

The meta-sedimentary rock samples yielded Nd T_{DM} model ages (Liew and Hofmann, 1988) in the interval between 2.46 Ga and 2.21 Ga, with εNd_t values ranging from 0.9 to +2.7 at the maximum depositional age for each sample (Fig. 8a). The Sm–Nd isotopic system is not extensively modified during diagenesis, metamorphism and sedimentation and the values obtained with this method represent the blend of the isotope signatures of the source rocks (McCulloch and Wasserburg, 1978). Therefore, it is possible to infer that the source area of São Vicente Complex meta-sedimentary rocks was composed mainly of Paleoproterozoic rocks with juvenile signatures, with secondary contributions from older crustal rocks. Older Nd T_{DM} model ages would have been associated with more negative εNd_t values, indicating contributions from older crustal rocks (Fig. 8a).

Thirty-eight previously dated zircons were analyzed for Lu–Hf isotopes, seventeen from the schist and gneisses (Fig. 9a) and twenty-one from the muscovite quartzites (Fig. 9b). All zircons have $^{176}Lu/^{177}Hf$ values of <0.002 and present-day $^{176}Hf/^{177}Hf$ values ranging from 0.2808 to 0.2816. The εHf_t data shows the predominance of Paleoproterozoic juvenile sources, with minor contributions from older crustal rocks (Fig. 9). Detrital zircons with juvenile signatures have εHf_t values ranging from +0.1 to +6.0 (U–Pb ages = 2099–2248 Ma; Hf T_{DM} ages = 2.74–2.47 Ga) and six crystals have lower εHf_t values of −9 to −0.3 indicating contributions from Archean and older Paleoproterozoic crustal rocks (U–Pb ages between 2113 and 2895 Ma, and Hf T_{DM} ages between 3.80 and 2.99 Ga).

6. Interlayered meta-basic rocks

Amphibolitic rocks occur as *boudins* in gneisses and are interlayered with quartzites and gneisses in metre-sized outcrops. Bulk rocks were analyzed for Nd isotopes and separated zircons were analyzed for U–Pb crystallization ages and Hf isotopic ratios. Sample C-509 has a predominance of crystal fragments with incipient internal zoning and rare prismatic or equidimensional crystals. Sample C-540 mostly contains prismatic zircon crystals with pyramidal terminations, magmatic internal zoning, with resorption textures (Corfu et al., 2004).

The results from sample C-509 are all crystallization ages that plot on a discordia with an upper intercept at 2136 ± 17 Ma and a lower intercept at 681 ± 170 Ma (n = 26; MSDW of 0.99) (Fig. 10a). Sample C-540 yielded two metamorphic rim ages (549 ± 14 Ma and 591 ± 14 Ma) and eleven crystallization ages aligned along a discordia with an upper intercept at 2143 ± 14 Ma and a lower intercept at 568 ± 14 Ma (MSDW of 1.5) (Fig. 10c). The lower intercepts are Neoproterozoic in age, and the C-540 sample lower intercept is similar to that obtained for the meta-sedimentary

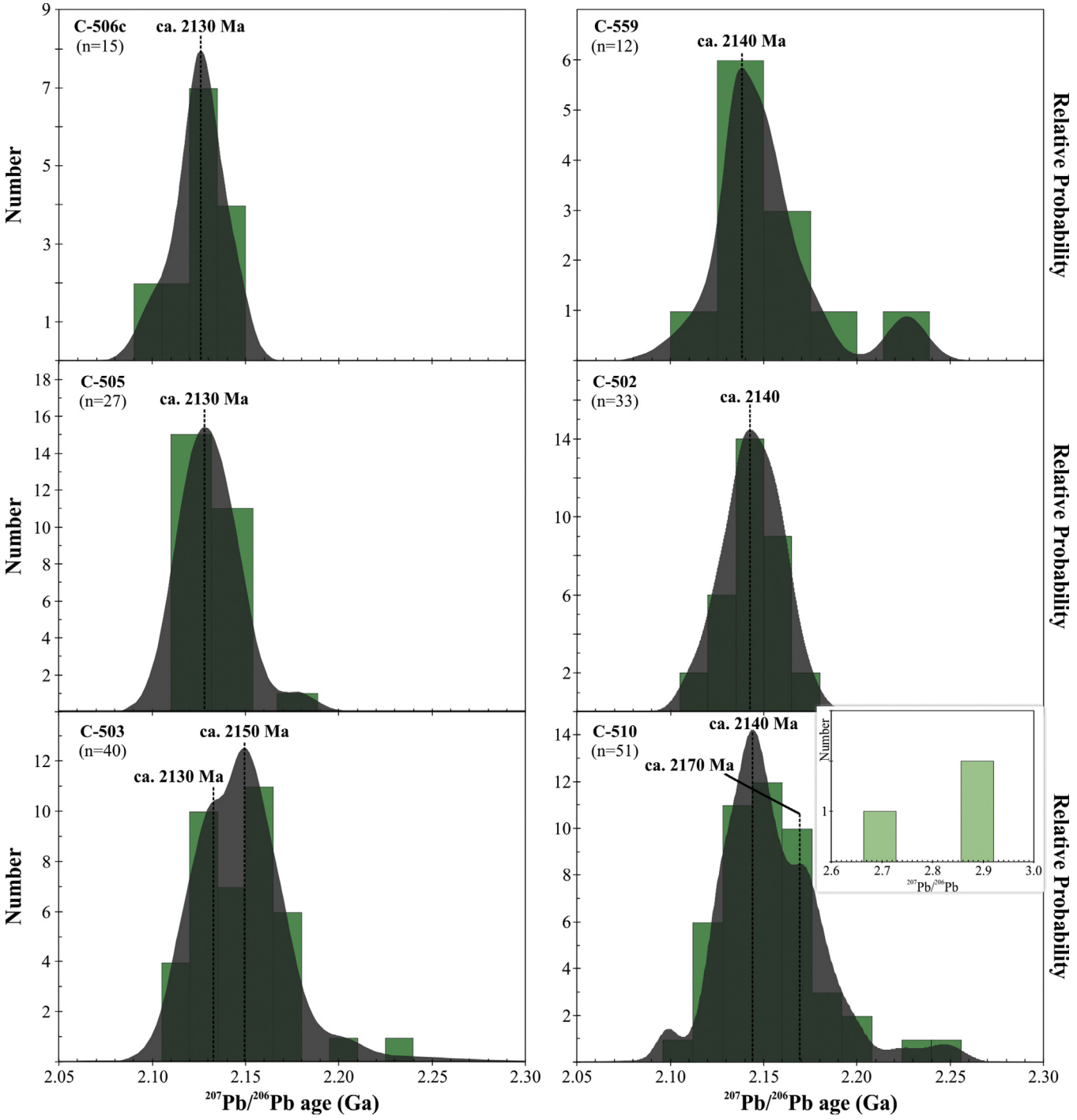

Fig. 7. U–Pb probability distribution plots of $^{207}Pb/^{206}Pb$ ages obtained in detrital zircons from three gneisses (C-502, C-503 and C-505), one schist (C-506c) and two quartzites (C-510 and C-559) of the São Vicente Complex. A key feature is the age peaks around 2100 Ma.

samples (594 ± 57 Ma) and for metamorphism in the passive margin allochthons (570–590 Ma). Therefore, the discordance, as for the meta-sedimentary rocks, is attributed to Pb loss during the Neoproterozoic tectonothermal event at ~590–570 Ma. Both upper intercept ages are considered to be the crystallization ages of these meta-basic rocks. Analogous ages between 2143 and 2158 Ma were reported by Pinheiro (2013) for three amphibolite samples, associated with the same units as those analyzed here.

Hf analyses were also performed on zircons from C-509 and they have present-day $^{176}Hf/^{177}Hf$ values between 0.28161 and 0.28167, with $^{176}Lu/^{177}Hf$ values of <0.001, and present-day εHf between −41 and −40. $^{176}Hf/^{177}Hf_t$ values are very similar for all crystals, ranging from 0.28158 to 0.28165. The εHf_t values were recalculated at the estimated crystallization age of 2136 Ma (Fig. 10a) and vary from +5.8 to +8.2, with Hf T_{DM} ages between 2.23 Ga and 2.38 Ga (Fig. 10b).

The bulk rock sample C-509 has the most juvenile Nd isotope signature, with $^{143}Nd/^{144}Nd$ of 0.51198, a Nd T_{DM} age of 2.19 Ga and εNd_{2136} of +3.4 (Fig. 8b). Sample C-540 has $^{143}Nd/^{144}Nd$ of 0.51225, a 2.35 Ga Nd T_{DM} age and εNd_{2143} of +2.3 (Fig. 8b).

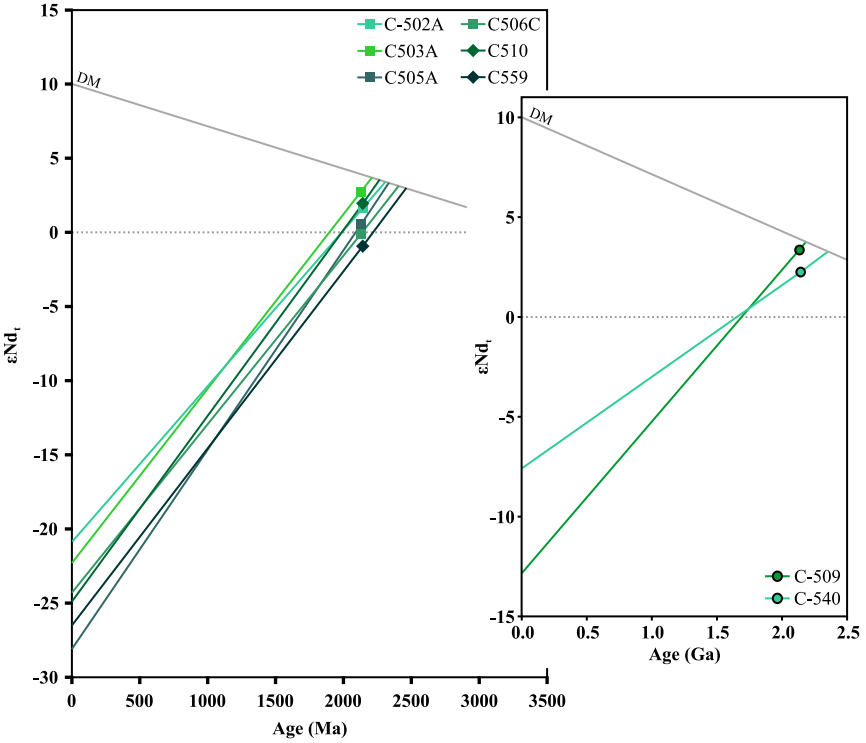

Fig. 8. Age (Ma) vs. εNd_t graph for the São Vicente Complex (a) meta-sedimentary and (b) meta-basic rocks. *t* is taken to be the maximum depositional age in (a) and the crystallization ages in (b). DM: Depleted mantle (Liew and Hofmann, 1988).

7. The intrusive Taguar gneissic granite

The Taguar gneissic granite intrudes the São Vicente Complex (Fig. 2). It is deformed, porphyritic and fine-grained, with igneous clinopyroxene partially replaced by hornblende (Vasconcellos, 1988). It is slightly peraluminous, with calc-alkaline to sub-alkaline affinity and it has a high $^{87}Sr/^{86}Sr$ initial ratio (ca. 0.7196). The zircons analyzed have upper and lower intercepts at 1726 ± 21 Ma and 615 ± 42 Ma, respectively (Fig. 11a and b). The older age is interpreted as the crystallization age of the rock. The younger age was obtained from three recrystallized rim analyses ($^{207}Pb/^{206}Pb$ ages: spot 6.1 = 543 ± 25 Ma; spot 26.2 = 608 ± 26 Ma; spot 27.2 = 589 ± 33 Ma). The lower intercept age is within error of the 594 Ma (meta-sedimentary samples) and 598 Ma (sample C-540) lower intercepts obtained for the São Vicente Complex samples, and the age of the 570–590 Ma metamorphism of the passive margin-related allochthons (Campos Neto et al., 2011; Machado et al., 1996; Valeriano et al., 2004).

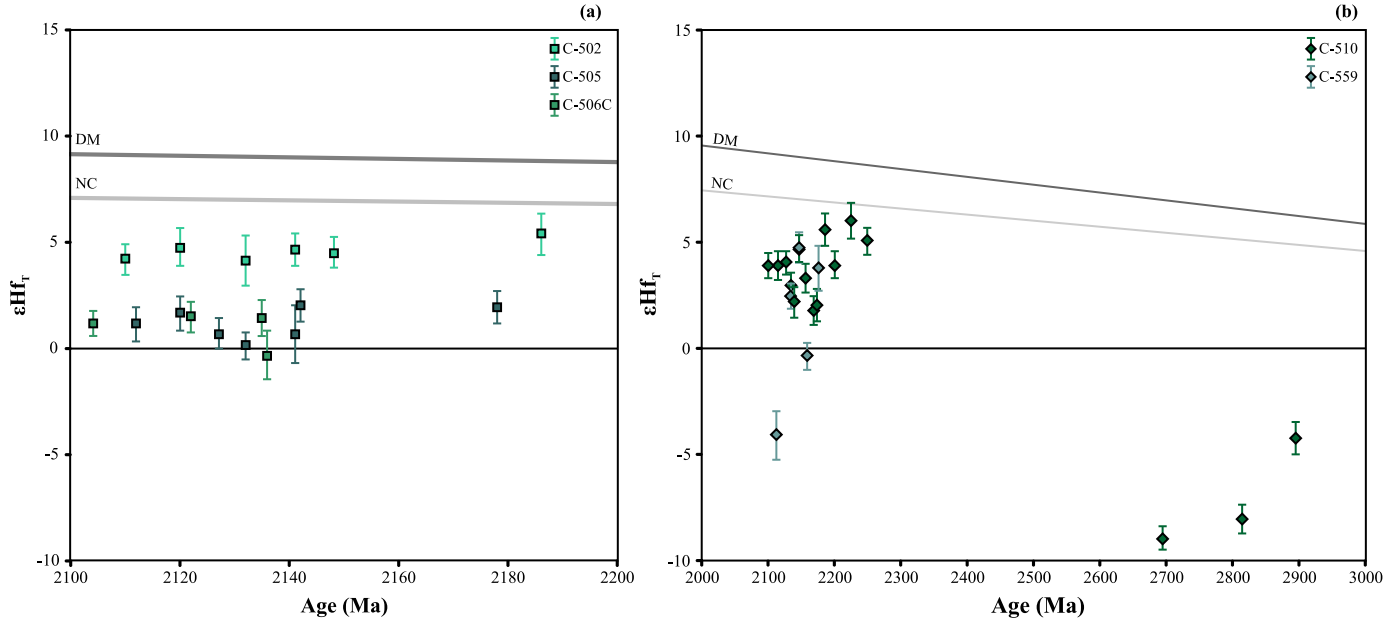

Fig. 9. (a) Age (Ma) vs. εHf_t graphs for the detrital zircons from the São Vicente Complex gneisses and schists; (b) Age (Ma) vs. εHf_t graphs for the detrital zircons from the São Vicente Complex muscovite quartzite samples. Note the different scales used, and the prevalence of juvenile Paleoproterozoic crystals over those with older crustal signatures. DM: Depleted mantle (Salters and Stracke, 2004; Workman and Hart, 2005); NC: new crust (Dhuime et al., 2011).

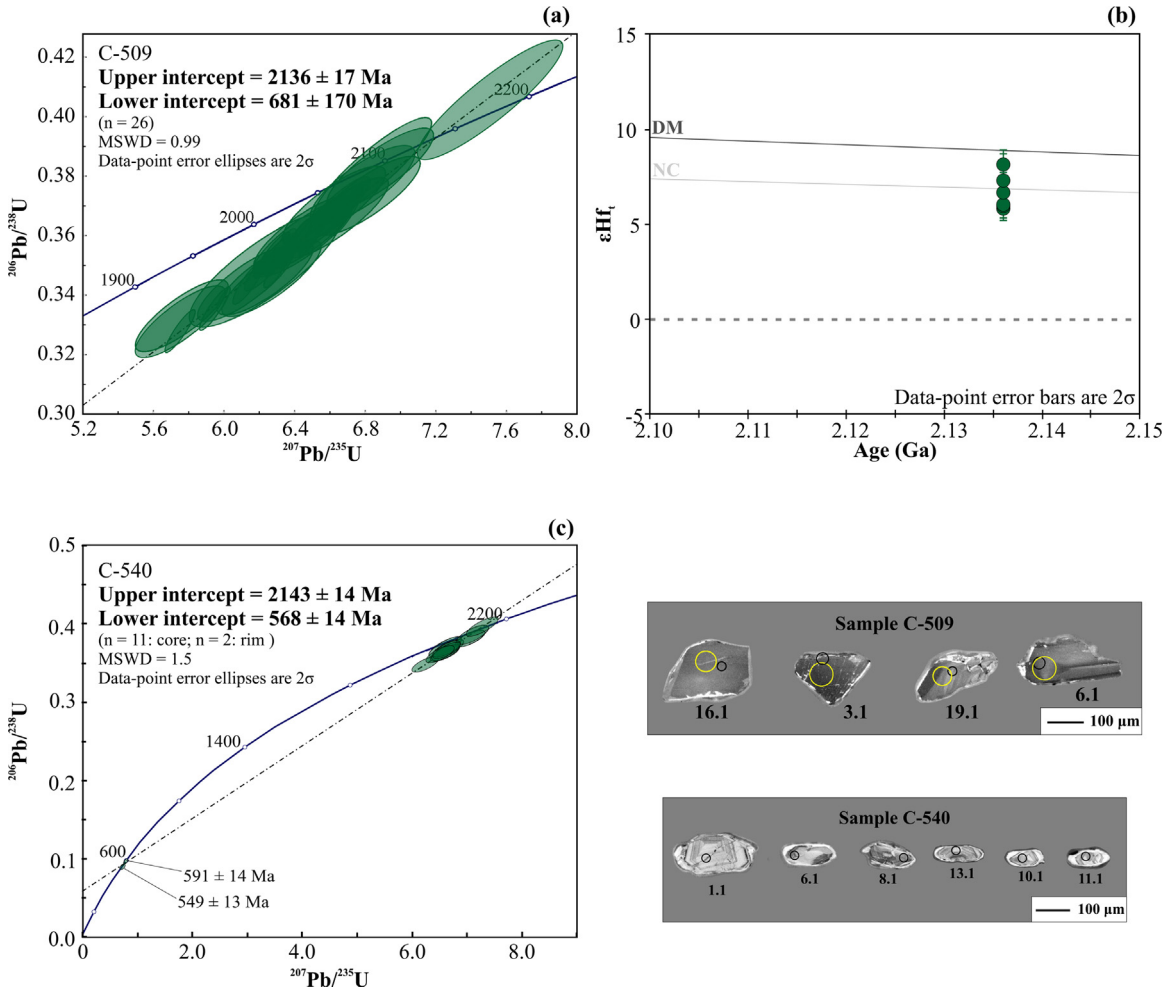

Fig. 10. (a) LA-MC-ICP-MS U–Pb Concordia diagram for sample C-509; (b) Age (Ga) vs. εHf_t graph for sample C-509; (c) LA-MC-ICP-MS U–Pb Concordia diagram for sample C-540. Note that representative zircon crystals of each sample show metamorphic overgrowth.

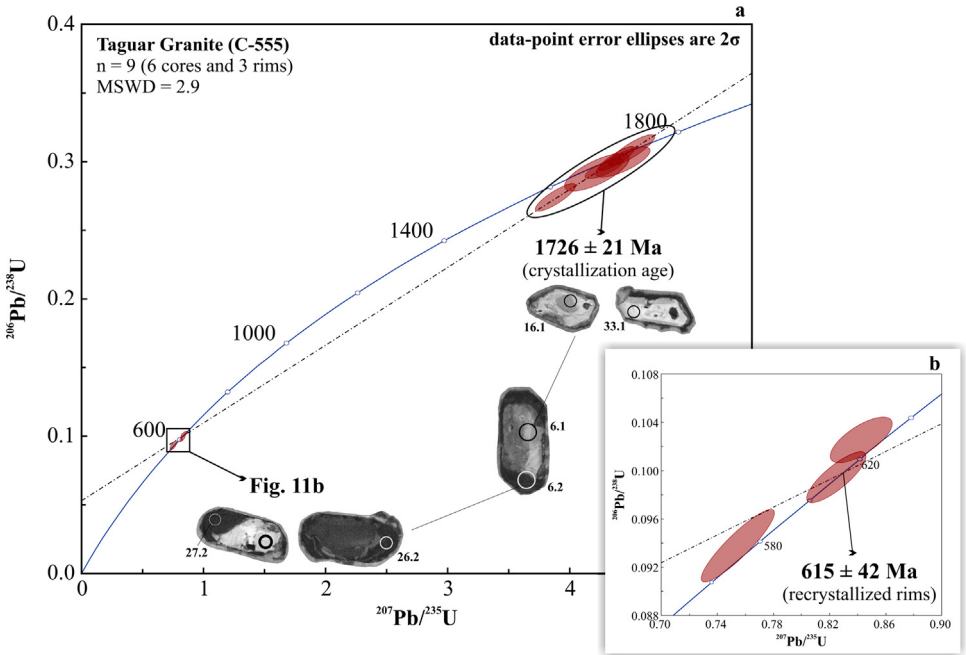

Fig. 11. (a) U–Pb Concordia diagram for zircons from the Taguar Granite (sample C-555) intrusive in the São Vicente Complex. The upper intercept ellipses ($n = 6$) correspond to crystallization ages and lower intercept ellipses ($n = 3$) correspond to recrystallization rim analyses; (b) U–Pb Concordia diagram showing only the rim analyses.

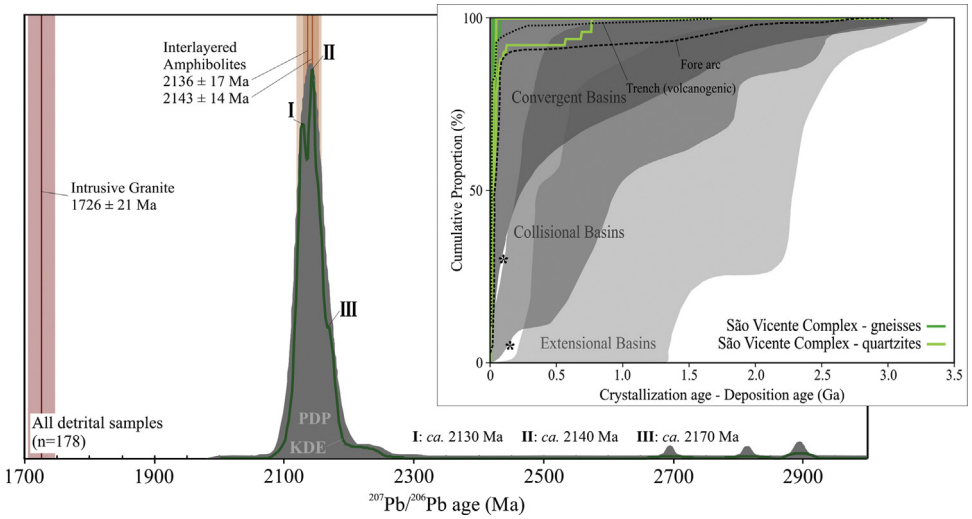

Fig. 12. (a) Probability Density Plot (PDP) and Kernel density estimate plot (KDE) showing all the detrital zircon ages obtained for the São Vicente Complex samples. Peaks I, II and III correspond to the three main age peaks of ca. 2130 Ma, 2140 Ma and 2170 Ma, respectively. Ages for the Taguar granite and the interlayered amphibolites are plotted for comparison; (b) (crystallization age – deposition age) vs. cumulative proportion graph (after Cawood et al., 2012) for zircons from gneisses, schist and quartzites belonging to the São Vicente Complex. Note that all samples plot in the active margin field similar to the fore arc and trench basins (* symbols: CA-DA < 150 Ma with a CP of 5% and CA-DA < 100 Ma with a CP of 30%).

8. Discussion

8.1. Age and isotopic signature of the sources

The crystallization ages of the detrital zircons are very restricted, with most ages being between 2185 and 2099 Ma. The meta-sedimentary samples yielded a Kernel density estimate (KDE) plot with three main age peaks of ca. 2170 Ma, 2140 Ma and 2130 Ma ($n = 178$) (Fig. 12a – age peaks I, II and III). The youngest age peak of ca. 2130 Ma is interpreted as the maximum depositional age of the São Vicente Complex.

There are also three crystals with Archean ages (2895 ± 7 Ma, 2894 ± 7 Ma and 2695 ± 10 Ma) and eight crystals with ages between 2248 Ma and 2190 Ma. Whole-rock Nd and detrital zircon εHf_t data from the meta-sedimentary rocks imply a juvenile signature for the dominant source (Nd T_{DM} = 2.31–2.21 Ga; εNd_t = +1.6 to +2.8; εHf_t = +0.1 to +6.0). Archean and ~2.2 Ga detrital zircons with negative εHf_t (−9 to −0.3) and meta-sedimentary samples with slightly positive and negative εNd_t values (−0.9 to +0.6; Nd T_{DM} = 2.46–2.33 Ga) provide evidence for minor contributions from an older crustal source.

8.2. Igneous rocks within the basin: limiting the period of sediment accumulation

Interlayered amphibolite rocks, found as *boudins* in sillimanite-garnet gneiss and m-sized outcrops, yielded U–Pb crystallization ages of 2136 ± 17 Ma and 2143 ± 14 Ma (Fig. 12a). The whole-rock Nd and zircon Hf data also indicate a juvenile signature for the meta-basic rocks, with εNd_t of +2.3 and +3.4 and εHf_t up to +8.2.

The amphibolite crystallization ages are very similar to the maximum depositional age of the associated sedimentary rocks, considering the associated errors, and thus they appear to represent syn-sedimentary magmatic activity. This reaffirms that the estimated maximum depositional age represents the sediment deposition age.

Deposition was in progress at least around 2143–2136 Ma and it lasted until after ca. 2130 Ma. The minimum depositional age is 1726 ± 21 Ma, the age of crystallization of the Taguar gneissic granite (Fig. 12a). This peraluminous gneissic granite is thought to represent a 1.7 Ga anorogenic A-type magmatism, strongly deformed during the Neoproterozoic orogeny (Vasconcellos, 1988). Therefore, the granite intrusion occurred when the São Vicente Complex was in a stable tectonic environment, consistent with the minimum age of deposition being older than 1.7 Ga.

8.3. Tectonic setting during deposition and crust generation

Approximately 90% of all the detrital zircon ages are within 50 Ma of the estimated sediment depositional age (Fig. 12b), a pattern that is associated with syn-sedimentary magmatism, and implies a convergent margin basin environment for the São Vicente Complex (Fig. 12b) (Cawood et al., 2012). The ages from the São Vicente Complex have similar age patterns to those attributed to trench volcanogenic and fore arc basin sediments (Fig. 12b), in that such settings are characterized by more than 30% of detrital zircon ages being less than 100 Ma older than the depositional age (Cawood et al., 2012).

The restricted range of detrital zircon ages, and the immature signature of the meta-sedimentary rocks demonstrated by the presence of lithic fragments and detrital K-feldspar, plagioclase and quartz granules, indicate that the source was close to the sedimentary basin. This reinforces the inferred convergent margin tectonic setting, and it is concluded that the São Vicente Complex meta-sedimentary rocks were deposited in an intra-arc tectonic setting with a juvenile magmatic arc as the main source of detrital zircons.

The mafic-ultramafic rock association and the similarities between the syn-sedimentary ages and the detrital age peaks, suggest an important site of juvenile magmatism, active for at least 40 Ma. The provenance data also indicate that new continental crust was generated at a juvenile magmatic arc, around 2.17–2.13 Ga.

8.4. Sources for the São Vicente Complex sediments

8.4.1. Pouso Alegre Complex

The Pouso Alegre Complex consists of granite and metatexitic tonalite to granodioritic orthogneisses (Figs. 2 and 3), and it has two main groups of U–Pb crystallization ages at 2070–2080 and 2140–2150 Ma (Campos Neto et al., 2011, 2004; Cioffi et al., 2016). The older ages resemble the ca. 2140 Ma detrital age peak attributed to the main source of the São Vicente basin (Fig. 12a – detrital age peak II) and they are similar to the 2136 and 2143 Ma

crystallization ages of the interlayered amphibolites obtained in this work (Figs. 10a and c). Cioffi et al. (2016) also obtained Paleoproterozoic Nd T_{DM} ages and juvenile whole-rock εNd_t and zircon εHf_t values for the Pouso Alegre orthogneisses, data that are similar to those obtained for the São Vicente Complex meta-sedimentary rocks. The Pouso Alegre Complex juvenile gneisses have arc-related chemical signatures and they have been interpreted as the youngest part of an arc complex (Cioffi et al., 2016) developed along the southern border of the São Francisco Paleoplate during 2.35–2.08 Ga (Mineiro belt – Ávila et al., 2010; Noce et al., 2000; Seixas et al., 2012; Teixeira et al., 2015, 2000). Therefore, we interpret the Pouso Alegre Complex as the juvenile magmatic arc that served as the main source for the São Vicente Complex meta-sedimentary rocks. Both complexes were already part of the southern edge of the São Francisco-Congo plate during the intrusion of the 1.7 Ga Taguar anorogenic granite and the assembly of West Gondwana in the Brasiliano/Pan-African Orogeny, serving as sources for early Neoproterozoic Lima Duarte and Carrancas passive margin basins.

8.4.2. Mineiro belt

Paleoproterozoic granitoids of the Mineiro belt with ages around 2100 Ma are common near the orogenic front and they are related to the Ritápolis Arc (2190–2120 Ma; Ávila et al., 2010; Noce et al., 2000; Teixeira et al., 2008). Despite similar ages the Ritápolis Arc is characterized by its crustal isotopic signature, suggesting that these granitoids were not the main source for the São Vicente Complex sediments. Tonalites, diorites and granites with ages between 2170–2150 Ma and 2140–2060 are also common on the SW portion of the Mineiro belt, however, its chemical and isotopic evidences of crustal contamination (Barbosa et al., 2015) make it an unlikely source. Older granitoids with juvenile isotope signatures (2230 Ma; Ávila et al., 2010; Teixeira et al., 2008) occur between Ritápolis Arc and the orogenic front, and so the São Vicente Complex would have been geographically distant from this arc at the time of deposition. The Alto Maranhão tonalite suite has juvenile isotopic signatures and ages of 2130–2120 Ma (Ávila et al., 2010; Noce et al., 2000; Seixas et al., 2013; Teixeira et al., 2008) and so it could also be regarded as a possible source. However, it is located north of Ritápolis Arc which makes it much less likely.

8.4.3. Juiz de Fora and Mantiqueira complexes

The Juiz de Fora Complex orthogranulites represent a calc-alkaline suite associated with convergent tectonic settings (Heilbron et al., 1998) and the basic rocks are tholeiites similar to island-arc and back-arc basalts (Costa, 1998; Noce et al., 2007). Inspite of its Ryacian age (2195–2084 Ma) and arc-related signature, it is interpreted as the basement of the Araçuaí orogen magmatic arc (item 2.2.2 – Noce et al., 2007; Pedrosa-Soares et al., 2008, 2001). Therefore, even though this complex satisfies the necessary age and isotope requirements to be a major source for the São Vicente Complex sedimentary basin, its paleogeographic position during the sedimentation of the São Vicente Complex is unknown.

The calc-alkaline orthogneisses of the Mantiqueira Complex are also Rhyacian in age but its protolith's Archean crustal signature (Heilbron et al., 2010; Noce et al., 2007) excludes these rocks as possible source.

9. Conclusions

- The São Vicente Complex meta-sedimentary rocks have immature characteristics and restricted detrital zircon ages, with three main age peaks of 2170 Ma, 2140 Ma and 2130 Ma;
- Whole-rock Nd T_{DM} model ages, positive εNd_t and positive εHf_t for detrital zircons indicate a juvenile signature for the dominant source of the sediments;
- Interlayered amphibolites yielded juvenile isotope ratios and crystallization ages of 2136 ± 17 Ma and 2143 ± 14 Ma;
- Amphibolite ages are similar to the youngest peak of detrital ages at 2130 Ma, which indicates that it represents syn-sedimentary magmatism and that the youngest detrital zircon ages approximate the depositional age of the meta-sedimentary rocks of the São Vicente Complex;
- Most of the ages of the detrital zircons ages are close to the age of the sediments, and such syn-sedimentary magmatism indicates a convergent margin basin for the São Vicente Complex meta-sedimentary samples. The pattern is similar to samples of fore arc and trench basins deposits elsewhere (Cawood et al., 2012).
- The evidence for a main source close to the basin (restricted detrital zircon ages and immature rocks) is consistent with a convergent plate margin, suggesting an intra-arc tectonic setting with a juvenile magmatic arc as the main source for the São Vicente Complex;
- Archean and ~2.2 Ga detrital zircons with enriched Hf isotope ratios indicate that there were also minor contributions from older crustal sources, mobilized by the evolution of the subduction system, or in a thin slice of old sialic crust associated with the juvenile arc;
- Sediment deposition was in progress around 2143–2136 Ma and it continued until after 2130 Ma;
- The minimum depositional age is older than 1726 ± 21 Ma, which is the crystallization age of the intrusive anorogenic Taguar gneissic granite. The intrusion occurred when the São Vicente Complex was in a stable tectonic environment;
- Mafic-ultramafic rock associations and the similarities between the amphibolite ages to detrital age peaks, suggest an important juvenile magmatism, active for at least 40 Ma;
- The results of this work highlight active continental crust generation along a juvenile magmatic arc, around 2.17–2.13 Ga;
- The Pouso Alegre Complex granite-granodioritic-tonalite orthogneisses with juvenile arc-related signature have been interpreted as the main source for the original sedimentary basin;
- The São Vicente and Pouso Alegre complexes were already part of the southern edge of the São Francisco-Congo plate during the intrusion of the 1.7 Ga Taguar granite and during the assembly of West Gondwana, serving as a source for Early Neoproterozoic Lima Duarte and Carrancas passive margin basins.

Acknowledgements

A. Westin and M.C. Campos Neto acknowledge support from São Paulo Research Foundation (FAPESP) through grants 2011/13311-9, 2013/13530-8 and 2013/19095-1. A. Westin is a grant holder at FAPESP and M. C. Campos Neto is a CNPq researcher. P. A. Cawood, C. J. Hawkesworth and H. Delavault acknowledge support from Natural Environment Research Council grant NE/J021822/1. Review and editorial handling by R. Parish and detailed review by W. Teixeira greatly helped to improve the manuscript. The authors also thank W. Sproesser and S. Souza for their assistance with the U–Pb analyses in the CPGeo-USP and B. Lima, E. Zacchi and F. V. Oliveira for their assistance in the GL-UnB.

Appendix A. Supplementary data

Supplementary data associated with this article can be found, in the online version, at http://dx.doi.org/10.1016/j.precamres.2016.02.004.

References

Alkmim, F.F., Brito-Neves, B.B., Barbosa, J.S.F., 1993. In: Dominguez, J.M.L., Misi, A. (Eds.), Arcabouço tectônico do Cráton do São Francisco – uma revisão. O Cráton Do São Francisco, Salvador, pp. 45–62.

Assumpção, M., Heintz, M., Vauchez, A., Silva, M.E., 2006. Upper mantle anisotropy in SE and Central Brazil from SKS splitting: evidence of asthenospheric flow around cratonic keel. Earth Planet. Sci. Lett. 250, 224–240.

Ávila, C.A., Teixeira, W., Bongiolo, E.M., Dussin, I.A., Vieira, T.A.T., 2014. Rhyacian evolution of subvolcanic and metasedimentary rocks of the southern segment of the Mineiro belt, São Francisco Craton, Brazil. Precambrian Res. 243, 221–251, http://dx.doi.org/10.1016/j.precamres.2013.12.028.

Ávila, C.A., Teixeira, W., Cordani, U.G., Moura, C.A.V., Pereira, R.M., 2010. Rhyacian (2.23–2.20 Ga) juvenile accretion in the southern São Francisco craton, Brazil: geochemical and isotopic evidence from the Serrinha magmatic suite, Mineiro belt. J. South Am. Earth Sci. 29, 464–482, http://dx.doi.org/10.1016/j.jsames.2009.07.009.

Barbarin, B., 1999. A review of the relationships between granitoid types, their origins and their geodynamic environments. Lithos 46, 605–626, http://dx.doi.org/10.1016/S0024-4937(98)00085-1.

Barbosa, N.S., Teixeira, W., Ávila, C.A., Montecinos, P.M., Bongiolo, E.M., 2015. 2.17–2.10 Ga plutonic episodes in the Mineiro belt, São Francisco Craton, Brazil: U–Pb ages, geochemical constraints and tectonics. Precambrian Res. 270, 204–225, http://dx.doi.org/10.1016/j.precamres.2015.09.010.

Basei, M.A.S., Frimmel, H.E., Nutman, A.P., Preciozzi, F., 2008. West Gondwana amalgamation based on detrital zircon ages from Neoproterozoic Ribeira and Dom Feliciano belts of South America and comparison with coeval sequences from SW Africa. Geol. Soc. Lond. Spec. Publ., 239–256, http://dx.doi.org/10.1144/SP294.13.

Bhatia, M.R., Crook, K.A.W., 1986. Trace element characteristics of graywackes and tectonic setting discrimination of sedimentary basins. Contrib. Miner. Pet. 92, 181–193.

Brito-Neves, B.B., Fuck, R.A., Cordani, U.G., Thomaz Filho, A., 1984. Influence of basement structures on the evolution of the major sedimentary basins of Brazil: a case of tectonic heritage. J. Geodyn. 1, 495–510.

Bühn, B., Pimentel, M.M., Matteini, M., Dantas, E.L., 2009. High spatial resolution analysis of Pb and U isotopes for geochronology by laser ablation multi-collector inductively coupled plasma mass spectrometry (LA-MC-ICP-MS). An. Acad. Bras. Cienc. 81, 99–114.

Campanha, G.A.C., Faleiros, F.M., Basei, M.A.S., Tassinari, C.C.G., Nutman, A.P., Vasconcelos, P.M., 2015. Geochemistry and age of mafic rocks from the Votuverava Group, southern Ribeira Belt, Brazil: evidence for 1490 Ma oceanic back-arc magmatism. Precambrian Res. 266, 530–550, http://dx.doi.org/10.1016/j.precamres.2015.05.026.

Campanha, G.A.C., Sadowski, G.R., 1999. Tectonics of the southern portion of the Ribeira Belt (Apiaí Domain). Precambrian Res. 98, 31–51, http://dx.doi.org/10.1016/S0301-9268(99)00027-3.

Campos Neto, M.C., 2000. Orogenic systems from southwestern Gondwana: an approach to Brasiliano-Pan African Cycle and orogenic collage in Southeastern Brazil. In: Cordani, U.G., Milani, E.J., Thomaz Filho, A., Campos, D.A. (Eds.), Tectonic Evolution of South America. Rio de Janeiro. , pp. 335–365.

Campos Neto, M.C., Basei, M.A.S., Janasi, V.A., Moraes, R., 2011. Orogen migration and tectonic setting of the Andrelândia Nappe system: an Ediacaran western Gondwana collage, south of São Francisco craton. J. South Am. Earth Sci. 32, 393–406.

Campos Neto, M.C., Basei, M.A.S., Vlach, S.R.F., Caby, R., Szabó, G.A.J., Vasconcelos, P., 2004. Migração de orógenos e superposição de orogêneses: um esboço da colagem brasiliana no sul do Cráton do São Francisco, SE – Brasil. Geol. USP – Série Científica 4, 13–40.

Campos Neto, M.C., Caby, R., 1999. Neoproterozoic high-pressure metamorphism and tectonic constraint from the nappe system south of the Sao Francisco Craton, southeast Brazil. Precambrian Res. 97, 3–26.

Campos Neto, M.C., Caby, R., 2000. Lower crust extrusion and terrane accretion in the Neoproterozoic nappes of southeast Brazil. Tectonics 19, 669–687.

Campos Neto, M.C., Cioffi, C.R., Moraes, R., Motta, R.G., Siga Jr., O., Basei, M.A.S., 2010. Structural and metamorphic control on the exhumation of high-P granulites: the Carvalhos Klippe example, from the oriental Andrelândia Nappe System, southern portion of the Brasília Orogen, Brazil. Precambrian Res. 180, 125–142, http://dx.doi.org/10.1016/j.precamres.2010.05.010.

Cawood, P.A., 1991. Characterisation of intra-oceanic magmatic arc source terranes by provenance studies of derived sediments. N. Z. J. Geol. Geophys. 34, 347–358.

Cawood, P.A., Hawkesworth, C.J., Dhuime, B., 2012. Detrital zircon record and tectonic setting. Geology 40, 875–878.

Cawood, P.A., Nemchin, A.A., 2001. Paleogeographic development of the east Laurentian margin: constraints from U–Pb dating of detrital zircons in the Newfoundland Appalachians. Geol. Soc. Am. Bull. 113, 1234–1246.

Cawood, P.A., Nemchin, A.A., Strachan, R., Prave, T., Krabbendam, M., 2007. Sedimentary basin and detrital zircon record along East Laurentia and Baltica during assembly and breakup of Rodinia. J. Geol. Soc. 164, 257–275.

Cioffi, C.R., Campos Neto, M.C., Möller, A., Rocha, B.C., 2016. Paleoproterozoic continental crust generation events at 2.15 and 2.08 Ga in the basement of the southern Brasília Orogen, SE Brazil. Precambrian Res. 275, 176–196, http://dx.doi.org/10.1016/j.precamres.2016.01.007.

Commission for the Geologial Map of the World, 2001. Geological Map of South America.

Condie, K.C., Beyer, E., Belousova, E., Griffin, W.L., O'Reilly, S.Y., 2005. U–Pb isotopic ages and Hf isotopic composition of single zircons: the search for juvenile Precambrian continental crust. Precambrian Res. 139, 42–100.

Cordani, U.G., Fuck, R.A., Thomaz Filho, A., Cunha, E.M.B., 1984. Estudo preliminar de integração do Pré-Cambriano com os eventos tectônicos das Bacias Sedimentares Brasileiras. Rev. Ciência-Técnica-Petróleo 15, 1–70.

Corfu, F., Hanchar, J.M., Hoskin, P.W.O., Kinny, P., 2004. Atlas of Zircon textures. In: Hanchar, J.M., Hoskin, P.W.O. (Eds.), Zircon – Reviews in Mineralogy and Geochemistry. , p. 500.

Costa, A.G., 1998. The granulite-facies rocks of the northern segment of the Ribeira Belt, eastern Minas Gerais, SE Brazil. Gondwana Res. 1, 367–372.

Cury, L.F., Kaulfuss, G.A., Siga Jr., O., Basei, M.A.S., Harara, O.M., Sato, K., 2002. Idades U–Pb (zircões) de 1.75 Ga em granitóides alcalinos deformados dos núcleos Betara e Tigre: evidências de regimes extensionais do Estateriano na Faixa Apiaí. Geol. USP – Série Científica 2, 95–108.

DePaolo, D.J., 1981. A neodymium and strontium study of the Mesozoic calc-alkaline granitic batholiths of the Sierra Nevada and Peninsular Ranges, California. J. Geophys. Res. – Solid Earth 86, 10470–10488.

Dhuime, B., Hawkesworth, C., Cawood, P., 2011. Geochemistry. When continents formed. Science 331, 154–155.

Dickinson, W.R., Gehrels, G.E., 2009. Use of U–Pb ages of detrital zircons to infer maximum depositional ages of strata: a test against a Colorado Plateau Mesozoic database. Earth Planet. Sci. Lett. 288, 115–125.

Dickinson, W.R., Suczek, C.A., 1979. Plate tectonics and sandstone composition. Am. Assoc. Pet. Geol. Bull. 63, 2164–2182.

Elhlou, S., Belousova, E., Griffin, W.L., Pearson, N.J., O'Reilly, S.Y., 2006. Trace element and isotopic composition of GJ-red zircon standard by laser ablation. Geochim. Cosmochim. Acta 70, A158, http://dx.doi.org/10.1016/j.gca.2006.06.1382.

Faleiros, F.M., Campanha, G.A.C., Martins, L., Vlach, S.R.F., Vasconcelos, P.M., 2011. Ediacaran high-pressure collision metamorphism and tectonics of the southern Ribeira Belt (SE Brazil): evidence for terrane accretion and dispersion during Gondwana assembly. Precambrian Res. 189, 263–291, http://dx.doi.org/10.1016/j.precamres.2011.07.013.

Fetter, A.H., Hackspacher, P.C., Ebert, H.D., Dantas, E.L., Costa, A.C.D., 2001. New Sm/Nd and U/Pb geochronological constraints on the Archean to Neoproterozoic evolution of the Amparo basement complex of the central Ribeira belt, Southeastern Brazil. In: III South American Symposium on Isotope Geology, Santiago, Chile. CD–ROM.

Fisher, C.M., Hanchar, J.M., Samson, S.D., Dhuime, B., Blichert-Toft, J., Vervoort, J.D., Lam, R., 2011. Synthetic zircon doped with hafnium and rare earth elements: a reference material for in situ hafnium isotope analysis. Chem. Geol. 286, 32–47.

Gehrels, G., 2013. Determining Max Depo Ages [WWW Document]. https://sites.google.com/a/laserchron.org/laserchron/home (accessed 01.01.15).

Gengo, R.M., (Unpublished Master's Dissertation) 2014. Petrologia de ortognaisses e granitóides do domínio Socorro, Nappe Socorro-Guaxupé, seção Extrema-Camanducaia. Instituto de Geociências, Universidade de São Paulo.

Hamilton, P.J., O'Nions, R.K., Bridgwater, D., Nutman, A., 1983. Sm–Nd studies of Archaean metasediments and metavolcanics from West Greenland and their implications for the Earth's early history. Earth Planet. Sci. Lett. 62, 263–272, http://dx.doi.org/10.1016/0012-821X(83)90089-4.

Hanchar, J.M., Hoskin, P.W.O. (Eds.), 2003. Zircon – Reviews in Mineralogy and Geochemistry. , 1st ed. Mineralogical Society of America and Geochemical Society.

Hawkesworth, C.J., Dhuime, B., Pietranik, A.B., Cawood, P.A., Kemp, A.I.S., Storey, C.D., 2010. The generation and evolution of the continental crust. J. Geol. Soc. Lond. 167, 229–248.

Hawkesworth, C.J., Kemp, A.I.S., 2006. Using hafnium and oxygen isotopes in zircons to unravel the record of crustal evolution. Chem. Geol. 226, 144–162.

Heilbron, M., Duarte, B.P., Nogueira, J.R., 1998. The Juiz de Fora Granulite Complex of the Central Ribeira Belt, SE Brazil: a Paleoproterozoic crustal segment thrust during the Pan-African Orogeny. Gondwana Res. 1, 373–381.

Heilbron, M., Duarte, B.P., Valeriano, C., de, M., Simonetti, A., Machado, N., Nogueira, J.R., 2010. Evolution of reworked Paleoproterozoic basement rocks within the Ribeira belt (Neoproterozoic), SE-Brazil, based on U–Pb geochronology: implications for paleogeographic reconstructions of the São Francisco-Congo paleocontinent. Precambrian Res. 178, 136–148, http://dx.doi.org/10.1016/j.precamres.2010.02.002.

Henrique-Pinto, R., Janasi, V.A., Vasconcellos, A.C.B.C., Sawyer, E.W., Barnes, S.-J., Basei, M.A.S., Tassinari, C.C.G., 2015. Zircon provenance in meta-sandstones of the São Roque Domain: implications for the Proterozoic evolution of the Ribeira Belt, SE Brazil. Precambrian Res. 256, 271–288, http://dx.doi.org/10.1016/j.precamres.2014.11.014.

Janoušek, V., Farrow, C.M., Erban, V., 2006. Interpretation of whole-rock geochemical data in igneous geochemistry: introducing Geochemical Data Toolkit (GCDkit). J. Pet. 47, 1255–1259.

Kemp, A.I.S., Foster, G.L., Scherstén, A., Whitehouse, M.J., Darling, J., Storey, C., 2009. Concurrent Pb-Hf isotope analysis of zircon by laser ablation multi-collector ICP-MS, with implications for the crustal evolution of Greenland and the Himalayas. Chem. Geol. 261, 244–260, http://dx.doi.org/10.1016/j.chemgeo.2008.06.019.

Lesquer, A., Almeida, F.F.M., Davino, A., Lachaud, J.C., Mailard, P., 1981. Signification Structurale des anomalies gravimetriques de la parte sud du Craton de Sao Francisco (Bresil). Tectonophysics 76, 273–293.

Liew, T.C., Hofmann, A.W., 1988. Precambrian crustal components, plutonic associations, plate environment of the Hercynian Fold Belt of central Europe: Indications from a Nd and Sr isotopic study. Contrib. Miner. Pet. 98, 129–138.

Ludwig, K.R., 2008. User's manual for Isoplot 3.70 – a geochronological toolkit for Microsoft Excel. Berkeley Geochronology Center. Special Publication, pp. 76.

Machado, N., Valladares, C., Heilbron, M., Valeriano, C., 1996. U–Pb geochronology of the central Ribeira belt (Brazil) and implications for the evolution of the Brazilian Orogeny. Precambrian Res. 79, 347–361.
Mantovani, M.S.M., Brito-Neves, B.B., 2005. The Paranapanema lithospheric block: its importance for Proterozoic (Rodinia, Gondwana) supercontinent theories. Gondwana Res. 8, 303–315.
Mantovani, M.S.M., Quintas, M.C.L., Shukowsky, W., Brito-Neves, B.B., 2005. Delimitation of the Paranapanema Proterozoic block: a geophysical contribution. Episodes 28.
McCulloch, M.T., Wasserburg, G.J., 1978. Sm–Nd and Rb–Sr chronology of continental crust formation – time of addition to continents of chemically fractionated mantle-derived materials are determined. Science 200, 1003–1011.
McLennan, S.M., Taylor, S.R., McCulloch, M.T., Maynard, J.B., 1990. Geochemical and Nd–Sr isotopic composition of deep-sea turbidites: crustal evolution and plate tectonic associations. Geochim. Cosmochim. Acta 54, 2015–2050.
Mora, C.A.S., Campos Neto, M.C., Basei, M.A.S., 2014. Syn-collisional lower continental crust anatexis in the Neoproterozoic Socorro-Guaxupé Nappe System, southern Brasília Orogen, Brazil: constraints from zircon U–Pb dating, Sr–Nd–Hf signatures and whole-rock geochemistry. Precambrian Res. 255, 847–864.
Navarro, M.S., Andrade, S., Ulbrich, H., Gomes, C.B., Girardi, V.A.V., 2008. The direct determination of rare earth elements in basaltic and related rocks using ICP-MS: testing the efficiency of microwave oven sample decomposition procedures. Geostand. Geoanal. Res. 32, 167–180.
Noce, C.M., Pedrosa-Soares, A.C., da Silva, L.C., Armstrong, R., Piuzana, D., 2007. Evolution of polycyclic basement complexes in the Araçuaí Orogen, based on U–Pb SHRIMP data: implications for Brazil-Africa links in Paleoproterozoic time. Precambrian Res. 159, 60–78.
Noce, C.M., Teixeira, W., Quéméneur, J.J.G., Martins, V.T.S., Bolzachini, É., 2000. Isotopic signatures of Paleoproterozoic granitoids from the southern Sao Francisco Craton and implications for the evolution of the Transamazonian Orogeny. J. South Am. Earth Sci. 13, 225–239.
Nunes, R.P.M., Trouw, R.A.J., Castro, E.O., 2008. Mapa Geológico – Varginha.
Oliveira, F.V., Oliveira, Í.L., Pivato Neto, L.A., Santos, R.V., Zacchi, E.N.P., Lima, B.A.F., Rodrigues, J.B., Dantas, E.L., Pimentel, M.M., 2014. Automation of LA-MC-ICPMS U–Pb data entry in in-house Excel spreadsheet using Visual Basic for Application (VBA). In: 9th South American Symposium on Isotope Geology, São Paulo, SP, p. 286.
Paciullo, F.V.P., Fonseca, A.C., Andreis, R.R., Ribeiro, A., Trouw, R.A., Wiedemann, C.M., 1996. Contribuição à geologia do sul de Minas Gerais edição das folhas 1:50.000 Itumirim, Itutinga, Madre de Deus, Luminárias. Minduri e Andrelândia. Anuário do Inst. Geociências 19, 123–142.
Paciullo, F.V.P., Ribeiro, A., Andreis, R.R., 1993. Reconstrução de uma bacia fragmentada: o caso do Ciclo Deposicional Andrelândia. In: II Simpósio Do Cráton Do São Francisco – Anais, Salvador, pp. 224–226.
Paciullo, F.V.P., Ribeiro, A., Andreis, R.R., Trouw, R.A.J., 2000. The Andrelândia Basin, a Neoproterozoic intraplate continental margin, southern Brasília Belt, Brazil. Rev. Bras. Geociências 30, 200–202.
Paciullo, F.V.P., Trouw, R.A.J., Ribeiro, A., Simões, L.A., Lopes r M., 2002. Mapa Geológico – Folha Andrelândia.
Patchett, P.J., Kouvo, O., Hedge, C.E., Tatsumoto, M., 1981. Evoltuion of continental crust and mantle heterogeneity: evidence from Hf isotopes. Contrib. Miner. Pet. 78, 279–297.
Pearce, J.A., Stern, R.J., 2006. Origin of back-arc basin magmas: trace element and isotope perspectives. In: Back-Arc Spreading Systems: Geological, Biological, Chemical and Physical Interactions.
Pedrosa-Soares, A.C., Alkmim, F.F., Tack, L., Noce, C.M., Babinski, M., Silva, L.C., Martins-Neto, M.A., 2008. Similarities and differences between the Brazilian and African counterparts of the Neoproterozoic Aracuai-West Congo orogen. In: Pankhurst, R.J., Trouw, R.A.J., de Brito Neves, B.B., Wit, M.J. (Eds.), West Gondwana: Pre-Cenozoic Correlations across the South Atlantic Region. The Geological Society of London, Special Publications, pp. 153–172, http://dx.doi.org/10.1144/SP294.9.
Pedrosa-Soares, A.C., Noce, C.M., Wiedemann, C.M., Pinto, C.P., 2001. The Araçuaí-West-Congo Orogen in Brazil: an overview of a confined orogen formed during Gondwanaland assembly. Precambrian Res. 110, 307–323, http://dx.doi.org/10.1016/S0301-9268(01)00174-7.
Peternel, R., Trouw, R.A.J., Schmitt, R., da, S., 2005. Interferência entre duas faixas móveis Neoproterozóicas: o caso das faixas Brasília e Ribeira no sudeste do Brasil. Rev. Bras. Geociências 35, 297–310.
Pinheiro, M.A.P., (Unpublished Master's Dissertation) 2013. Geologia e petrogênese de corpos máfico- ultramáficos da Faixa Brasília Sul, borda sul do Cráton São Francisco – MG. Universidade Federal de Ouro Preto.
Pupin, J.P., 1980. Zircon and granite petrology. Contrib. Miner. Pet. 73, 207–220.
Pupin, J.P., 2000. Granite genesis related to geodynamics from Hf–Y in zircon. Trans. R. Soc. Edinb. Earth Sci. 91, 245–256.
Quéméneur, J.J.G., Ribeiro, A., Paciullo, F.V.P., Heilbron, M., Trouw, R.A.J., Valença, J.G., Noce, C.M., 2002. Mapa Geológico – Folha Lavras.
Ribeiro, A., Paciullo, F.V.P., Noce, C.M., Valeriano, C.M., Valença, J.G., Ávila, C.A., Trouw, R.A.J., Silva, M.A., 2002. Mapa Geológico – Folha São João del Rei.
Ribeiro, A., Teixeira, W., Dussin, I.A., Ávila, C.A., Nascimento, D., 2013. U–Pb LA-ICP-MS detrital zircon ages of the São João del Rei and Carandaí basins: new evidence of intermittent Proterozoic rifting in the São Francisco paleocontinent. Gondwana Res. 24, 713–726.
Ribeiro, A., Trouw, R.A.J., Andreis, R.R., Paciullo, F.V.P., Valença, J.G., 1995. Evolução das bacias Proterozóicas e o termo-tectonismo Brasiliano na margem sul do Cráton do São Francisco. Rev. Bras. Geociências 25, 235–248.
Rocha, M.P., Schimmel, M., Assumpção, M., 2011. Upper-mantle seismic structure beneath SE and Central Brazil from P- and S-wave regional traveltime tomography. Geophys. J. Int. 184, 268–286, http://dx.doi.org/10.1111/j.1365-246X.2010.04831.x.
Salters, V.J.M., Stracke, A., 2004. Composition of the depleted mantle Geochemistry. Geophys. Geosyst. 5, Q05B07, http://dx.doi.org/10.1029/2003GC000597.
Santos, C.A., (Unpublished Master's Dissertation) 2014. Geologia, petrografia e geocronologia dos gnaisses e rochas associadas na região entre Carrancas, Minduri e Luminárias (MG). Instituto de Geociências, Universidade de São Paulo.
Santos, P.S., (Unpublished Master's Dissertation) 2011. Geocronologia, área-fonte e ambiente tectônico da unidade Santo Antônio – Megassequência Andrelândia. Instituto de Geociências, Universidade Federal do Rio de Janeiro.
Sato, K., Basei, M.A.S., Siga Jr., O., Onoi, A.T., 2010. In situ U-Th-Pb isotopic analyses by excimer laser ablation/ICP-MS on Brazilian megacrystal xenotime: first results of U–Pb isotoper at CPGeo-IG-USP. In: VII South American Symposium on Isotope Geology, Brasília – DF, pp. 349–352.
Segal, I., Halicz, L., Platzner, I.T., 2003. Accurate isotope ratio measurements of ytterbium by multiple collection inductively coupled plasma mass spectrometry applying erbium and hafnium in an improved double external normalization procedure. J. Anal. At. Spectrom. 18, 1217–1223.
Seixas, L.A.R., Bardintzeff, J.-M., Stevenson, R., Bonin, B., 2013. Petrology of the high-Mg tonalites and dioritic enclaves of the ca. 2130 Ma Alto Maranhão suite: evidence for a major juvenile crustal addition event during the Rhyacian orogenesis, Mineiro Belt, southeast Brazil. Precambrian Res. 238, 18–41, http://dx.doi.org/10.1016/j.precamres.2013.09.015.
Seixas, L.A.R., David, J., Stevenson, R., 2012. Geochemistry, Nd isotopes and U–Pb geochronology of a 2350 Ma TTG suite, Minas Gerais, Brazil: implications for the crustal evolution of the southern São Francisco craton. Precambrian Res. 196-197, 61–80, http://dx.doi.org/10.1016/j.precamres.2011.11.002.
Siga Jr., O., Cury, L.F., McReath, I., Ribeiro, L.M., de, A., Sato, K., Basei, M.A.S., Passarelli, C.R., 2011. Geology and geochronology of the Betara region in south-southeastern Brazil: evidence for possible Statherian (1.80–1.75 Ga) and Calymmian (1.50–1.45 Ga) extension events. Gondwana Res. 19, 260–274.
Siivola, J., Schmid, R., 2007. List of Mineral abbreviations – Recommendations by the IUGS Subcommission on the Systematics of Metamorphic Rocks [WWW Document]. IUGS web version 01.02.07. www.bgs.ac.uk/scmr/docs/papers/paper_12.pdf (accessed 28.04.15).
Stacey, J.S., Kramers, J.D., 1975. Approximation of terrestrial lead isotope evolution by a two-stage model. Earth Planet. Sci. Lett. 26, 207–221.
Sun, S., McDonough, W.F.-s., 1989. Chemical and isotopic systematics of oceanic basalts: implications for mantle composition and processes. Geol. Soc. Lond. Spec. Publ. 42, 313–345.
Tassinari, C.C.G., Nutman, A.,2001. Archean and Proterozoic multiple tectonothermal events recorded by gneisses in the Amparo Region, São Paulo state, Brazil. In: III South American Symposium on Isotope Geology. Sociedad Geológica de Chile, Pucón, Chile, pp. 252–254.
Taylor, S.R., McLennan, S.M., 1985. The Continental Crust: Its Composition and Evolution. Blackwell Scientific, Oxford.
Teixeira, W., Ávila, C.A., Dussin, I.A., Corrêa Neto, A.V., Bongiolo, E.M., Santos, J.O., Barbosa, N.S., 2015. A juvenile accretion episode (2.35–2.32 Ga) in the Mineiro belt and its role to the Minas accretionary orogeny: zircon U–Pb–Hf and geochemical evidences. Precambrian Res. 256, 148–169.
Teixeira, W., Ávila, C.A., Nunes, L.C., 2008. Nd–Sr isotopic geochemistry and U–Pb geochronology of the Fé Granitic Gneiss and Lajedo Granodiorite: implications for Paleoproterozoic evolution of the Mineiro Belt, Southern São Francisco Craton, Brazil. Rev. do Inst. Geociências 8, 53–74.
Teixeira, W., Sabatè, P., Barbosa, J., Noce, C.M., Carneiro, M.A., 2000. Archean and Paleoproterozoic evolution of the São Francisco Craton, Brazil. In: Cordani, U.G., Milani, E.J., Thomaz Filho, A., Campos, D.A. (Eds.), Tectonic Evolution of South America. 31 International Geological Congress Rio de Janeiro. , pp. 101–137.
Trouw, R.A.J., Heilbron, M., Ribeiro, A., Paciullo, F.V.P., Valeriano, C.M., Almeida, J.C.H., Tupinambá, M., Andreis, R.R., 2000. The central segment of the Ribeira Belt. In: Cordani, U.G., Milani, E.J., Thomaz Filho, A., Campos, D.A. (Eds.), Tectonic Evolution of South America. 31 International Geological Congress Rio de Janeiro. , pp. 335–365.
Trouw, R.A.J., Nunes, R.P.M., Trouw, C.C., Matos, G.C., 2008. Mapa Geológico – Folha Itajubá.
Trouw, R.A.J., Paciullo, F.V.P., Ribeiro, A., Bittar, S., Almeida, J.C.H., 2002. Mapa Geológico – Folha Caxambu.
Ussami, N., 1999. Estruturação e limites da placa litosférica São Franciscana: Contribuição Gravimétrica – Tese de livre docência. Universidade de São Paulo.
Valeriano, C.M., Machado, N., Simonetti, A., Valladares, C.S., Seer, H.J., Simões, L.S.A., 2004. U–Pb geochronology of the southern Brasília belt (SE-Brazil): sedimentary provenance, Neoproterozoic orogeny and assembly of West Gondwana. Precambrian Res. 130, 27–55.
Valladares, C.S., Machado, N., Heilbron, M., Gauthier, G., 2004. Ages of detrital zircon from siliciclastic successions south of the São Francisco Craton, Brazil: implications for the evolution of Proterozoic basins. Gondwana Res. 7, 913–921.
Vasconcellos, A.C.B.C., (Unpublished Master's Dissertation) 1988. Grupo Andrelândia na região de Ouro Fino, MG. Instituto de Geociências, Universidade de São Paulo.
Vermeesch, P., 2012. On the visualisation of detrital age distributions. Chem. Geol. 312–313, 190–194, http://dx.doi.org/10.1016/j.chemgeo.2012.04.021.

Vervoort, J.D., Patchett, P.J., Söderlund, U., Baker, M., 2004. Isotopic composition of Yb and the determination of Lu concentrations and Lu/Hf ratios by isotope dilution using MC-ICPMS. Geochem. Geophys. Geosyst. 5, Q11002.

Vinagre, R., Trouw, R.A.J., Mendes, J.C., Duffles, P., Peternel, R., Matos, G., 2014. New evidence of a magmatic arc in the southern Brasília Belt Brazil: the Serra da Água Limpa batholith (Socorro-Guaxupé Nappe). J. South Am. Earth Sci. 54, 120–139.

Westin, A., Campos Neto, M.C., 2013. Provenance and tectonic setting of the external nappe of the Southern Brasília Orogen. J. South Am. Earth Sci. 48, 220–239.

Woodhead, J.D., Hergt, J.M., 2001. Strontium, neodymium and lead isotope analyses of NIST glass certified reference materials: SRM 610, 612, 614. Geostand. Newsl. 25, 261–266, http://dx.doi.org/10.1111/j.1751-908X.2001.tb00601.x.

Workman, R.K., Hart, S.R., 2005. Major and trace element composition of the depleted MORB mantle (DMM). Earth Planet. Sci. Lett. 231, 53–72, http://dx.doi.org/10.1016/j.epsl.2004.12.005.

Zuquim, M.P.S., Trouw, R.a J., Trouw, C.C., Tohver, E., 2011. Structural evolution and U–Pb SHRIMP zircon ages of the Neoproterozoic Maria da Fé Shear Zone, central Ribeira Belt – SE Brazil. J. South Am. Earth Sci. 31, 199–213.